Journal Pre-proof

Design, synthesis and biological evaluation of quinoxaline compounds as anti-HIV agents targeting reverse transcriptase enzyme

Lucas Fabian, Marisa Taverna Porro, Natalia Gomez, Melina Salvatori, Gabriela Turk, Dario Estrin, Albertina Moglioni

PII: S0223-5234(19)31139-0

DOI: https://doi.org/10.1016/j.ejmech.2019.111987

Reference: EJMECH 111987

To appear in: *European Journal of Medicinal Chemistry*

Received Date: 18 September 2019

Revised Date: 21 November 2019

Accepted Date: 17 December 2019

Please cite this article as: L. Fabian, M. Taverna Porro, N. Gomez, M. Salvatori, G. Turk, D. Estrin, A. Moglioni, Design, synthesis and biological evaluation of quinoxaline compounds as anti-HIV agents targeting reverse transcriptase enzyme, *European Journal of Medicinal Chemistry* (2020), doi: https://doi.org/10.1016/j.ejmech.2019.111987.

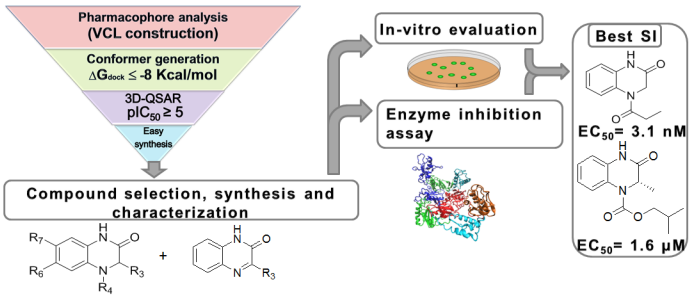

Design, synthesis and biological evaluation of quinoxaline compounds as anti-HIV agents targeting reverse transcriptase enzyme

Lucas Fabian[a,b,§], Marisa Taverna Porro[b,§], Natalia Gomez[c], Melina Salvatori[d], Gabriela Turk[d], Dario Estrin[e], Albertina Moglioni[a,b]*

[a] *Cátedra de Química Medicinal, Facultad de Farmacia y Bioquímica, Universidad de Buenos Aires, CABA, 1113, Argentina*
[b] *Instituto de la Química y Metabolismo del Fármaco (IQUIMEFA), CONICET-Universidad de Buenos Aires, CABA, 1113, Argentina*
[c] *Instituto de Investigaciones Farmacológicas (ININFA),CONICET-Universidad de Buenos Aires, CABA, 1113, Argentina*
[d] *Instituto de Investigaciones Biomédicas en Retrovirus y Sida (INBIRS), CONICET-Universidad de Buenos Aires, CABA, 1113, Argentina*
[e] *Instituto de Química Física de los Materiales, Medio Ambiente y Energía (INQUIMAE), Facultad de Ciencias Exactas y Naturales, CONICET-Universidad de Buenos Aires, CABA,1428 , Argentina*

§ Both authors contributed equally

Keywords

Quinoxaline synthesis, reverse transcriptase, virtual chemical library, anti-HIV agents

Highlights

- A quinoxaline library was constructed and evaluated using docking and 3D-QSAR.
- Twenty-five quinoxaline derivatives were selected and synthesized.
- All compounds were screened for their *in vitro* RT inhibitory activity.
- Four compounds were evaluated as anti-HIV agents in infected MT2 cells.
- Compounds **12** and **3** showed promising anti-HIV activities.

Abstract

Infection by human immunodeficiency virus still represents a continuous serious concern and a global threat to human health. Due to appearance of multi-resistant virus strains and the serious adverse side effects of the antiretroviral therapy administered, there is an urgent need for the development of new treatment agents, more active, less toxic and with increased tolerability to mutations. Quinoxaline derivatives are an emergent class of heterocyclic compounds with a wide spectrum of biological activities and therapeutic applications. These types of compounds have also shown high potency in the inhibition of HIV reverse transcriptase and HIV replication in cell culture. For these reasons we propose, in this work, the design, synthesis and biological evaluation of quinoxaline derivatives targeting HIV reverse transcriptase enzyme. For this, we first carried out a structure-based development of target-specific compound virtual chemical library of quinoxaline derivatives. The rational construction of the virtual chemical library was based on previously assigned pharmacophore features. This library was processed by a virtual screening protocol employing molecular docking and 3D-QSAR. Twenty-five quinoxaline

compounds were selected for synthesis in the basis of their docking and 3D-QSAR scores and chemical synthetic simplicity. They were evaluated as inhibitors of the recombinant wild-type reverse transcriptase enzyme. Finally, the anti-HIV activity and cytotoxicity of the synthesized quinoxaline compounds with highest reverse transcriptase inhibitory capabilities was evaluated. This simple screening strategy led to the discovery of two selective and potent quinoxaline reverse transcriptase inhibitors with high selectivity index.

1. Introduction

Infection by human immunodeficiency virus (HIV) still represents a continuous serious concern and a global threat to human health and has important social and economic consequences all over the world. Nowadays, 37 million people are living with HIV and still around 1 million people annually dies from AIDS related illness [1]. Despite the outstanding advances in the treatment of HIV infection, AIDS remains an incurable disease. The side effects due to daily use and elevated drug toxicity promotes reduced patient adherence. This, in addition to the high replication rate of HIV, favors the appearance of multi-resistant HIV strains [2]. For these reasons AIDS treatment is still chemotherapeutically challenging and, therefore, there is an urgent need for the development of new agents that are more active, less toxic and with increased tolerability to mutations.

Combination antiretroviral therapy (cART) is required for durable virologic suppression. One of the most frequent targets in cART is the HIV reverse transcriptase enzyme (RT), since its reverse transcription step is essential in viral replication and it is not present in humans. Non-nucleoside RT inhibitors (NNRTIs) have become an important ingredient of the cART schemes, which includes nevirapine, delavirdine, efavirenz, etravirine, and rilpivirine approved for clinical use [3]. However, their efficiency has been undermined by the appearance of drug resistant variants of HIV and therefore it is necessary to design novel drugs to cope with resistance [4]. Quinoxaline derivatives are a versatile class of heterocyclic compounds with a wide spectrum of biological activities and therapeutic applications [5]. Compounds containing a quinoxaline scaffold have shown high potency as NNRTIs and in the inhibition of HIV-1 replication in cell culture [6]. Derivatives such as HBY [7], HBQ [8] and S-2720 [9], efavirenz (EFV) [10] and quinoline U-78036 [11] and UC38 [12] (Figure 1) are examples of quinoxaline and related compounds with RT inhibitory action.

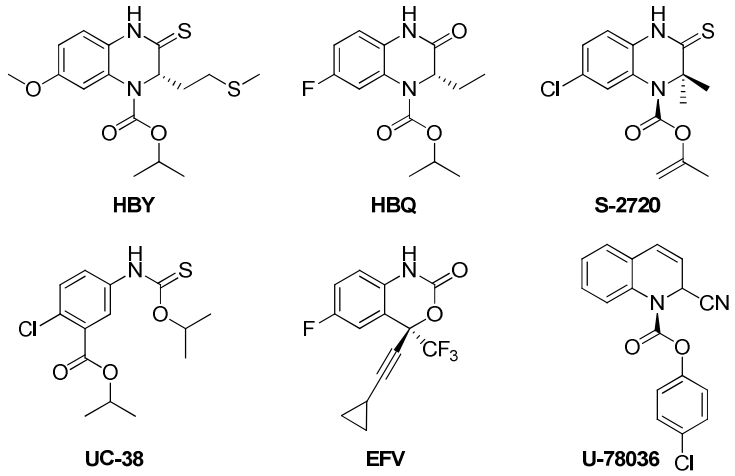

Figure 1. Quinoxaline structures and structurally related compounds with RT inhibitory activity.

The development of novel NNRTIs using Computer Aided Drug Design (CADD) is well documented in literature [13-16]. Approaches employing a combination of virtual screening and *de-novo* design based on QSAR studies, docking and molecular dynamics have been successful in the discovery of new and active NNRTIs [17-19]. Particularly, Patel et al [20] have designed novel quinoxaline derivative inhibitors of HIV integrase by a two-ligand based drug design approach using pharmacophore modelling and 3D-QSAR. These compounds were chosen by their docking scores, synthesized and biologically evaluated, resulting in two derivatives with IC_{50} in the micromolar range. In this context, we developed a virtual screening protocol employing molecular docking and 3D-QSAR in order to predict the NNRTI activity of different families of compounds [21, 22]. This methodology allowed us to successfully predict the RT inhibitory activity of 58 quinoxaline compounds, whose IC_{50} had previously been described in the literature.

In the present study, based on the previously developed computational approach, we carried out the design, synthesis and biological evaluation of quinoxaline derivatives targeting HIV RT. For this aim, we first carried out a structure-based development of target-specific compound virtual chemical library of quinoxaline derivatives. The screening of the virtual chemical library using the protocol previously described (docking and 3D-QSAR) [21, 22] resulted in the preparation of twenty-five quinoxaline with potential as RT inhibitors. These were selected on the basis of their calculated IC_{50} values and their chemical synthetic simplicity, and then evaluated as RT inhibitors and as anti-HIV agents in infected cells.

2. Results and discussion

2.1 Virtual chemical library construction and screening

To construct a virtual chemical library of quinoxaline (VCL) compounds with potential RT inhibitory activity, we needed first to define the most important structural requirements for their interaction with the enzyme allosteric site. Structural knowledge was obtained from the two-dimensional pharmacophore model developed previously by Wang [13], and more specifically, from ligand–protein complexes of related compounds, as shown in Figure 2. For the latter, we took into account quinoxaline and related

compounds (Figure 1) that were equally represented into the three-featured pharmacophore. This analysis revealed that the important chemical features to identify novel RT inhibitors were: a five- or six-membered aromatic ring; a five- to seven-membered ring which can either be aromatic or aliphatic and a hydrophilic center that can be nitrogen, oxygen, or sulfur.

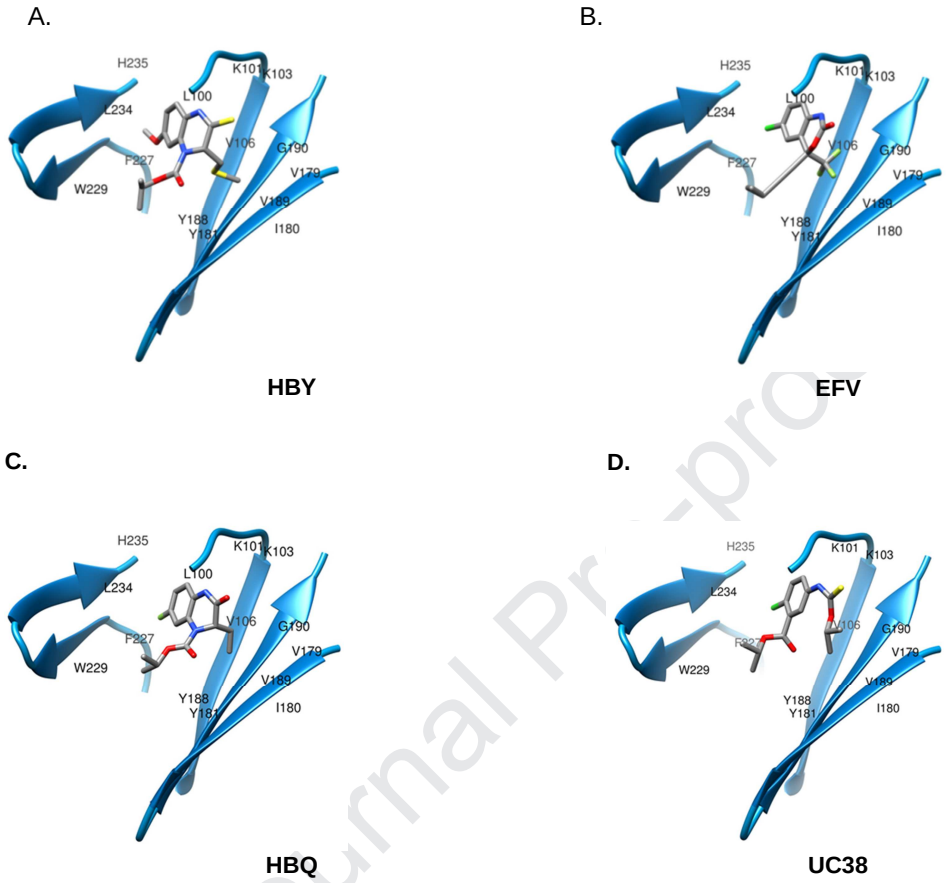

Figure 2. Different structures of the RT ligand binding domain bound to different NNRTIs containing a quinoxaline or quinoxaline related scaffold: A. HBY, B.EFV, C. HBQ and D. UC38. The RT structure is reported in blue and the residues relevant to ligand binding are labeled on top.

Thus, the quinoxaline VCL was constructed by combining different substituents, namely R_3, R_3', R_4, R_6 y R_7 (contemplating also both stereochemistries at position 3 of the heterocyclic ring), with tQNX and dQNX structures as scaffolds (Table 1). Alkyl or aromatic chains in positions 3 and 4, small substituents in positions 6 and 7, and a hydrogen forming bond group at position 1 and 2 were, as previously mentioned, the most important features taken into account. The residues selected as possible substituents at positions 3, 4, 6 and 7 are shown in Table 1. The VCL was finally constructed by combining the SMILES strings of the different substituents with those of tQNX and dQNX scaffolds (Table 1). All the possible combinations of the proposed residues gave rise to a VCL composed by a total of 45804 quinoxaline or related compounds that were further evaluated in the screening step.

Table 1. Substituents at positions 3, 4, 6 and 7.

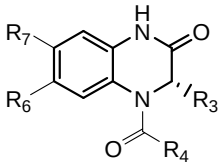

1,2,3,4-tetrahydroquinoxalin-2-one (tQXN)

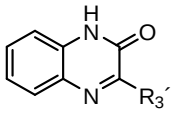

1,2-dihydroquinoxalin-2-one (dQNX)

R_3	
H	methyl
(methylthio)ethyl	2-butyl
isopropyl	isobutyl

R_3'			
H	methyl	(methylthio)ethyl	2-butyl
isopropyl	isobutyl	2-carboxy ethyl	2-carboxy ethyl, ethyl ester
benzyl	hydroxyl	2-carboxy ethyl, methyl ester	2-carboxy ethyl, isopropyl ester

R_4			
methyl	pent-3-in-1-yl	3,3-dimethyl-pentyl	4-chloro-2-butenyl
ethyl	pent-4-in-1-yl	2,2-dimethyl-pentyl	4-fluor-2-butenyl
propyl	1-methyl-2-en-	2-propen-1-yl	3-phenyl-propyl
butyl	2-cyclopropyl-ethyl	2-buten-1-yl	benzyl
pentyl	cyclopentyl	3-buten-1-yl	2-amine-1-ethyl
hexyl	Isopropyl	2-methyl-3-buten-1-yl	2-cyano-1-ethyl
heptyl	2-butyl	(*Z*)-penta-2,4-dien-1-yl	phenacyl
octyl	Isobutyl	3-cyclopenten-1-yl	4-methoxy-phenacyl
nonyl	terbutyl	cyclobutyl-methyl	4-nitro-phenacyl
decyl	2-pentyl	cyclopropyl-methyl	4-chloro-phenacyl
cyclopropyl	3-pentyl	cyclohexyl-methyl	4-methyl-phenacyl
cyclobutyl	isopentyl	2-chloro-ethyl	4-bromo-phenacyl
cyclopentyl	neopentyl	3-chloro-propyl	4-hydroxy-phenacyl
cyclohexyl	2-hexyl	2-chloro-propyl	2-nitro-phenacyl
2,4-dien-cyclopentyl	3-hexyl	4-chloro-butyl	2-chloro-phenacyl
2,5-dien-cyclohexyl	3,3-dimethyl-butyl	3-chloro-butyl	2-methyl-phenacyl
propen-2-in-1-yl	2,2-dimethyl-butyl	2-trifluoromethyl-ethyl	2-methoxy-phenacyl
buten-2-in-1-yl	2,3-dimethyl-butyl	3-bromo-propyl	benzhydryl
buten-3-in-1-yl	3,4-dimethyl-pentyl	4-bromo-butyl	2-thienyl
penta-2-in-1-yl	4,4-dimethyl-pentyl	3-bromo-butyl	2-thienyl-methyl
formyl	isopropyloxycarbonyl	phenylacetyl	4-chloro-thiophenesulfonyl
acetyl	difluoroacetyl	4-methoxy-phenylacetyl	thiophenesulfonyl
propionyl	4-methoxybenzoyl	4-nitrophenylacetyl	1-naphtalenesulfonyl
butanoyl	phenylpyruvate	3-chloro-thiophene-2-carbonyl	4-amine-benzoyl
chloroacetyl	2-nitrobenzoyl	4-chloro-thiophene-2-carbonyl	2-hydroxy-benzoyl
3-chloro-propanoyl	3-nitrobenzoyl	(furan-2-yl)-acetyl	isonicotinohydrazide-*N*'-yl
benzoyl	4-nitrobenzoyl	(3-chloro-furan-2-yl)-acetyl	3-isopropylurea-1-yl
benzenesulfonyl	2-chlorobenzoyl	(*E*)-3-(furan-3-yl) acryloyl	acetamide-*N*-yl
2-butyl-oxy-carbonyl	3-chlorobenzoyl	nicotinate	aniline-*N*-yl
bromoacetyl	4-chlorobenzoyl	isonicotinate	dihydrocinnamoyl
2-methyl-acryloyl	acryloyl	4-methyl-benzenesulfonyl	3-methoxy-benzenesulfonyl
benzyloxycarbonyl	thiophene-2-carbonyl	3-chloro-benzenesulfonyl	thiophene-3-carbonyl

R_6 / R_7					
H	chloro	fluor	methyl	acetylamine	amine

The chemical library screening was performed using two stages: docking and 3D-QSAR, as previously described [21, 22]. Briefly, the 3D structures of all the VCL members were generated from their SMILES isomeric notations followed by geometry optimization. Subsequently, molecular docking was used to generate the ligand conformers that served as input for WHIM descriptors calculation, using the PDB ID 2B6A RT structure as template. This protein was selected as the ligand conformer generating template from a previous cross-docking calibration experiment and showed to be the most efficient for crystallographic pose prediction among a strucurally diverse set of compounds. Only the best scoring docking pose of those VCL compounds with the lowest ΔG_{dock} values with a cutoff of $\Delta G_{dock} \leq -8.0$ Kcal/mol were selected as conformers for further analysis. This cutoff was selected as it was the average value found for active compounds in the calibration steps.This constraint allowed us the selection of a total of 14792 compounds (approximately 30% of the VCL). Afterwards, these structures were evaluated by means of the 3D-QSAR model shown in equation 1, together with WHIM descriptors obtained in the previous step. In this way, the half maximal inhibitory concentration (IC_{50}) values were calculated.

$$\mathbf{pIC_{50} = 3.18 * E3m + 5.06 * E2u + 4.4 * Dv - 0.72} \qquad \text{Equation 1}$$

From the 14792 compounds enlisted in the VCL, a total of 2970 showed a pIC_{50} higher than 5 (6.5% of the initial VCL). Structural analysis of the 2970 compounds that met both docking and 3D-QSAR criteria showed that the chemical nature of substituents at position 6 and 7 didn't play a significant role in the calculated inhibitory effect. For this reason, quinoxaline derivatives not bearing substituents at these positions were chosen to be synthesized from commercial and inexpensive *o*-halonitrobenzene and/or *o*-phenylenediamine. Chemical variability was achieved by introduction of a wide variety of substituents at positions 3 and 4 of the heterocyclic system. Their synthetic simplicity was also considered, as some compounds with the highest predicted pIC_{50} showed to be synthetically challenging. Taking all these into account, twenty-five quinoxaline and/or quinoxaline related compounds (**1**-**25**, Figure 3) with predicted pIC_{50} values within the range of actual active compounds (4.93-8.65) were chosen to be chemically prepared and evaluated as RT inhibitors. The ΔG_{dock}, WHIM coefficient descriptors and predicted pIC_{50} values determined for the synthesized compounds are shown in Table 2.

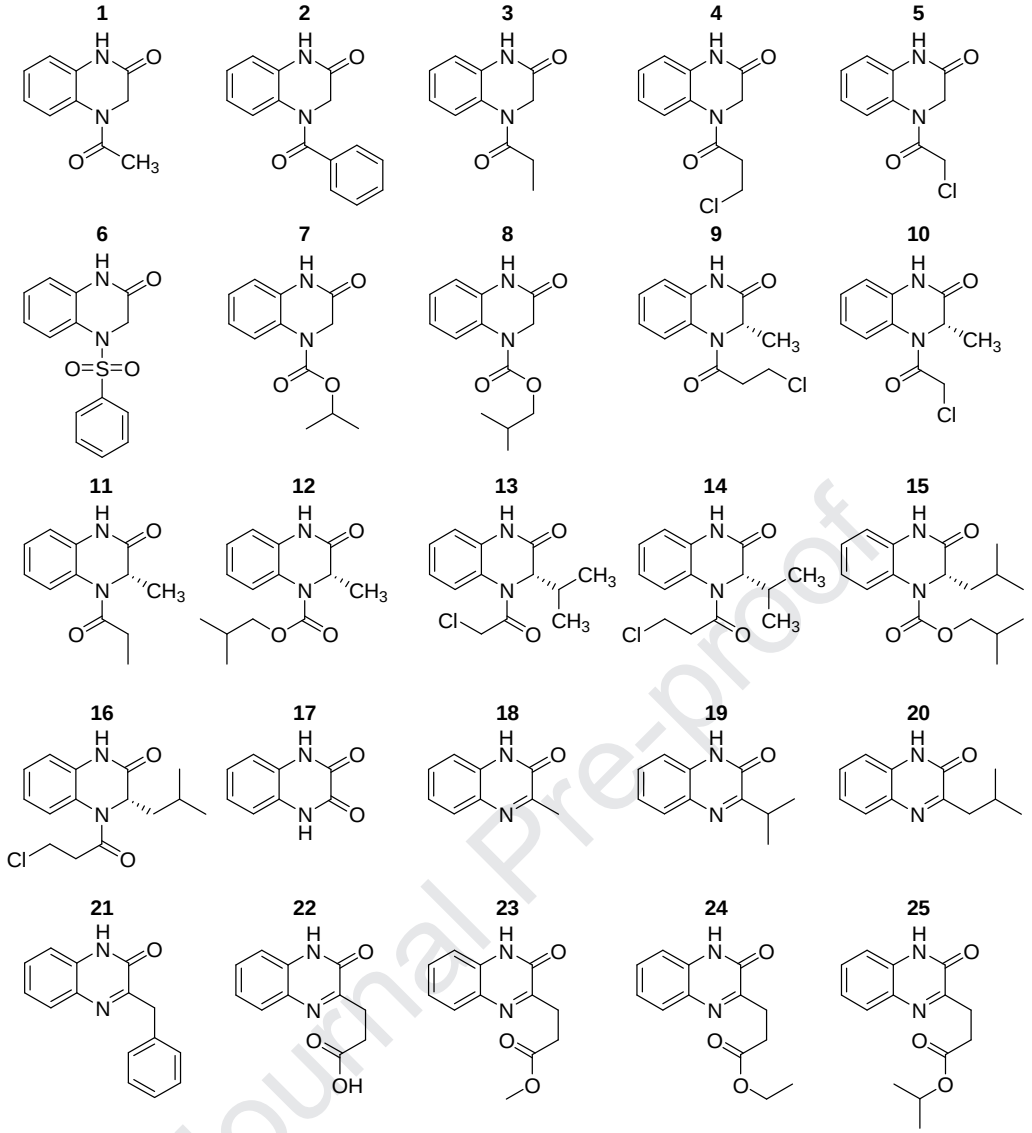

Figure 3. Synthesized quinoxaline and related compounds.

Table 2. ΔG_{dock}, predicted pIC_{50} and WHIM coefficient descriptors determined for compounds **1-25.**

Compound #	ΔG_{dock}	pIC_{50}cal	E3m	Dv	E2u
1	-11.7	6.11	0.060	0.897	0.533
2	-8.5	6.12	0.136	0.952	0.439
3	-8.2	5.68	0.063	0.882	0.458
4	-9.3	8.18	0.372	1.118	0.552
5	-9.1	8.01	0.401	1.004	0.600
6	-10.6	8.65	0.400	1.220	0.540
7	-10.4	7.23	0.212	1.100	0.482
8	-10.6	6.44	0.102	1.058	0.430
9	-8.3	8.05	0.330	1.111	0.560
10	-10.5	6.21	0.071	1.041	0.420
11	-8.9	5.77	0.088	0.897	0.448
12	-8.9	6.46	0.146	1.048	0.416

13	-11.4	7.16	0.216	1.165	0.409
14	-10	6.99	0.245	1.048	0.458
15	-11.6	7.30	0.331	1.107	0.414
16	-9.8	7.33	0.274	1.120	0.444
17	-10.2	7.00	0.148	0.989	0.573
18	-11.2	4.93	0.002	0.694	0.512
19	-9.6	5.19	0.037	0.811	0.440
20	-9.3	5.26	0.052	0.849	0.410
21	-10.8	5.82	0.041	0.878	0.504
22	-10.2	6.52	0.230	0.934	0.475
23	-10.9	8.25	0.175	1.220	0.601
24	-10.5	7.40	0.221	1.049	0.553
25	-9.4	7.24	0.099	1.086	0.566

ΔG_{dock}: Gibbs free energy calculated with AutodockVina 1.0 program. pIC_{50}cal: biological activity calculated using model 1 expressed as log $1/IC_{50}$ where IC_{50} is in Molar unit. WHIM descriptors: E2u, component eta 2 weighted at connectivity; E3m, component eta 3 weighted at mass; Dv, non-directional global descriptor weighted for molecular volume.

*2.2. Synthesis of quinoxaline and quinoxaline related compounds (**1-25**)*

2.2.1. 1,2,3,4-tetrahydroquinoxalin-2-ones (**tQNXs**)synthesis(**1**-**16**)

The 1,2,3,4-tetrahydroquinoxalin-2-ones (tQNXs) derivatives **1-16** (Figure 3) bearing different substituents at positions 3 and 4 were prepared according to general Scheme 1. In general, commercially available *o*-halonitrobenzene was reacted with the corresponding α-amino acid (bearing the substituents at position 3) through an aromatic nucleophilic substitution reaction. Then, by nitro reduction and further cyclization, the acyclic intermediate (**a**, Scheme 1) gave rise to the corresponding heterocyclic secondary amines (**b**, Scheme 1). Finally, the different 4-substituted tQNXs derivatives were prepared by *N*-acylation of the heterocyclic amines with the corresponding acyl chlorides.

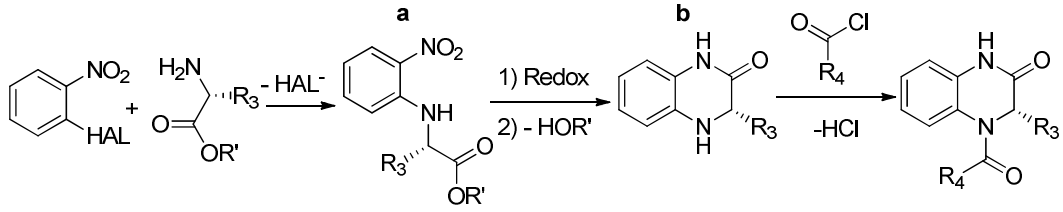

Scheme 1. General synthetic scheme for the preparation of *N*4-acylated tQNXs.

Microwave (MW) assisted methods were developed for the first synthetic step. MW assisted synthesis provides cheaper and cleaner chemistry, enhanced reaction rates and higher yields. Optimum reaction conditions were initially determined by using α-amino acid methyl esthers as nucleophiles and two halonitrobenzenes: 1-fluoro-2-nitrobenzene (FNB) and 1-chloro-2-nitrobenzene (ClNB) [23]. The nucleophilic displacement reaction gave higher reaction rates yields using as substrate FNB than ClNB

(Table 3). Due to the fact that other authors have described the obtention of these derivatives by means of a modification of the Sanger reaction [24], in which they directly use the free amino acid as starting material, we decided to evaluate these MW-assisted nucleophilic displacement reactions using as nucleophiles the potassium salts of the α-amino acids. The yields and rates obtained were similar independently of the amino acid starting material employed. For this reason, we decided to continue with the *N*-arylsubstituted intermediates preparation using directly the potassium salt of the corresponding α-amino acids, giving rise to the different products with yields around 60 %.

Recently, graphene has shown great potential as an alternative solid carbocatalyst for a variety of MW-assisted catalyzed reactions [25-28]. Therefore, in order to increase the observed yields and reaction rates, we decided to evaluate the incorporation of graphene to the displacement reaction. The heterogeneous system was reacted as a suspension of the solid catalyst and halonitrobenzene in a potassium carbonate solution of the free α-amino acids. The adittion of graphene as catalyst in this MW-assisted reaction greatly increased the reaction rate and yields, obtaining the *N*-arylsubtituted intermediates with around 90 % yield in only 15 minutes reaction time, while products were obtained in much lower yields without the addition of this catalyst (for comparison reactions with glycine see Table 4). This optimized one-pot methodology allowed us to obtain with high yields (approx. 90%) the nitro derivatives **ND1**-**ND8** (Figure 4), by means of reaction between amino acids such as glycine, (S)-alanine, (S)-valine and (S)-leucine and their corresponding methyl esters with commercial FNB.

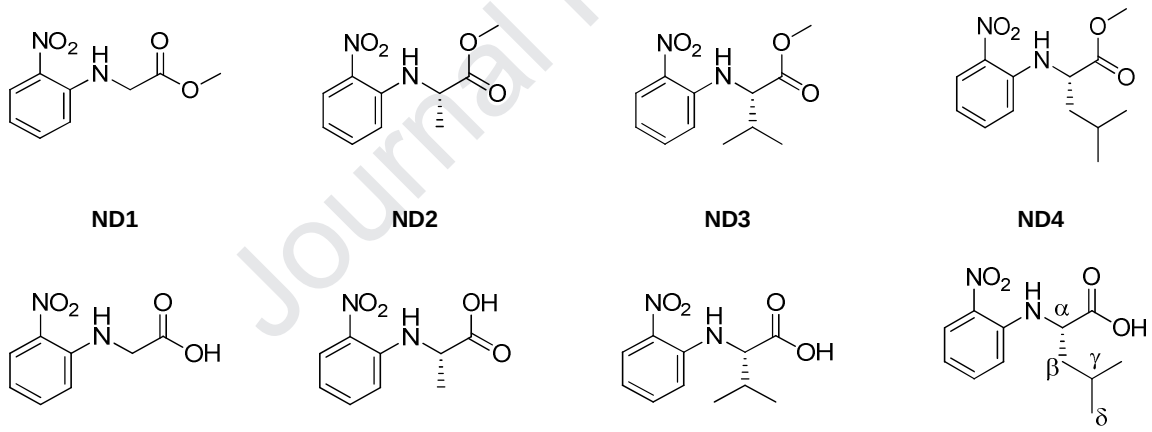

Figure 4. *N*-nitrophenyl derivatives (ND) obtained from amino acids and their methyl esters.

Table 3. Yields and reaction times for the preparation of the acyclic synthesis intermediates of TQNXs.

Amino acid derivative	2-ClNB		2-FNB		2-FNB + graphene	
	Time (min)	Yield (%)	Time (min)	Yield (%)	Time (min)	Yield (%)
Potassium glycinate	40	45	30	75	15	90
Glycine methyl ester	40	50	30	80	15	90

The preparation of the tQNXs by reduction of the NDs (**ND1-8**, Figure 4) has already been reported in literature [29-30] using different reducing agents such as $HCOONH_4$/Pd-C; $Na_2S_2O_3/K_2CO_3$; $SnCl_2$/HCl or Zn^0/HCl. These works showed that while reducing the nitro group, partial cyclization of the intermediate aniline was also simultaneously taking place and that the complete conversion of the acyclic intermediate to the tQNXs could be achieved by means of heating [24]. In this context, the reduction of the nitro group followed by the subsequent cyclization reaction was evaluated using: $HCOONH_4$/Pd-C and $SnCl_2$/HCl. The first reducing agent produced a mixture of products including cyclized compounds with different oxidation degrees. On the other hand, reduction with $SnCl_2$ in acidic medium and subsequent heating led to the cyclized hydrochlorides tQNXs as major products. Using the latter experimental conditions, compounds **tQNX1**, **tQNX2, tQNX3** and **tQNX4** were prepared (Figure 5).

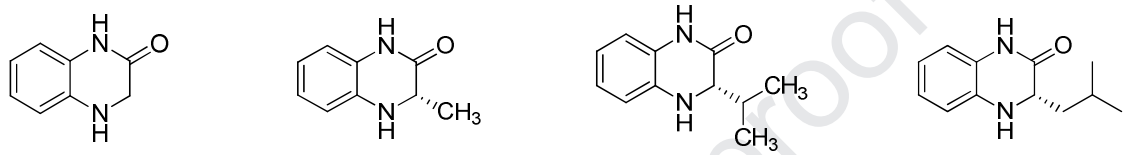

tQNX 1 **tQNX 2** **tQNX 3** **tQNX 4**

Figure 5.Chemical structures of prepared tQNXs.

N-acylation of **tQNX1** (Figure 5) with different acylating agents such as acetyl and propionyl chloride, β-chloro propanoyl chloride, isobutyl chloroformate, among others, led to derivatives **1**-**8** (Figure 3) with very good yields. The general reaction conditions involved the use of the corresponding acyl chloride in a slight stequiometric excess, using ethyl acetate or acetonitrile as solvents and hexamethylenetetramine or triethylamine as base. Analogously, the acylation of the derivatives **tQNX 2**, **3** and **4** led to derivatives **9**-**16** (Figure 3) with high yields.

2.2.2 Quinoxalin-2-ones (**dQNXs**) synthesis (**17**-**25**)

The preparation of the quinoxalin-2-ones (**dQNXs**) derivatives with a variety of substituents at position 3 was carried out according to different synthetic approaches.

Compounds **17, 18, 21** and **22** (Figure 3) were prepared as shown in Scheme 2, by condensation of *o*-phenylenediamine with the corresponding α-keto acids. The optimization of this synthetic approach using MW-assisted methodologies has already been reported by us [31]. Using the previously optimized conditions, high yields (approx. 90 %) were obtained using equimolar amounts of the reactants and a minimum amount of solvent (ethanol).

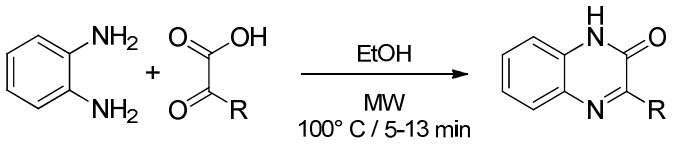

Scheme 2. General synthetic scheme for the preparation dQNXs.

Compounds **23, 24** and **25** (Figure 3) were obtained by MW-assisted esterification of compound **22** with the corresponding alcohol using methanesulfonic acid supported on alumina as catalyst, also as previoulsy reported by us [23].

Finally, dQNXs **19** and **20** (Figure 3) were prepared by hydrogen peroxidation of **tQNX3** and **tQNX4** (Figure 5), respectively.

*2.3 Evaluation of the RT inhibitory activity of compounds **1**-**25***

In order to determine if the synthesized quinoxaline compounds **1**-**25** (Figure 3) acted as RT inhibitors, we performed an initial screening of their *in-vitro* RT inhibitory activity at two concentrations: 10 µM and 100 µM. The activity of the expressed wild-type enzyme was optimized for RT activity by measuring dTTP incorporation on a poly(rA)-oligo(dT) template primer duplex. HIV-1 RT was presented in the reaction at a final concentration of 50 nM. The commercial NNRTI nevirapine (NVP) was included as a positive control. The inhibition percentages relative to the wild-type enzymatic activity of the twenty-five quinoxaline derivatives evaluated were calculated are summarized in Table 5. Most compounds evaluated showed inhibitory capabilities at the highest concentration tested in this assay (100 µM). Also, six of the evaluated quinoxalines presenting the higher inhibitory activity values were considered as hit compounds (**1**, **3**, **8**, **12**, **15** and **20**, Figure 3). Compound **3** (Figure 3) was a particularly interesting derivative, since it exhibited a potent inhibitory activity at both of the concentrations evaluated, with values comparable to the commercial compound NVP.

The results presented in Table 4 show that introduction of isobutyl substituents on the quinoxaline amide nitrogen atom (R_4) seems to cause an increase in the RT inhibitory potency (compounds **8**, **12** and **15**, Figure 3) regardless of the identity of the susbtituent at position 3, while with other subtituents at this position (R_4), the presence of diverse residues at position 3 were detrimental for the inhibitory activity. For instance, at 100 µM, the potent inhibitory activity of compound **3** (99% of inhibition) was greatly diminished by the introduction of a methyl residue at position 3 (compound **11**, 23 % of inhibition). The same behaviour was observed when comparing the inhibition percentages between unsubstituted compound **5** (32 % of inhibition) with the corresponding values of compounds with alkyl subtituents at position 3, compounds **10** (8 % inhibition) and **13** (12 % of inhibition). All of the observed results are in agreement with the theoretical pharmacophore characterization proposed by Wang and also by us (see 2.1).

Table 4. Percentage RT inhibition by compounds **1-25**.

	% RT Inhibition	
Comp. #	100 µM	10 µM
NVP	**98**	**91**
1	**56**	**7**
2	33	14
3	**99**	**91**
4	26	12
5	32	24
6	12	14
7	19	20
8	46	20
9	28	15
10	8	8
11	23	7
12	**64**	**37**
13	12	5
14	7	7
15	**51**	**22**
16	20	10
17	1	8
18	1	3
19	17	12
20	**73**	**15**
21	26	10
22	15	20
23	23	8
24	12	15
25	25	21

The four most active compounds (**3, 12, 15** and **20**, Table 4, Figure 3) were chosen for further analysis. Assesment of the inhibition of RT activity was repeated using a wider range of concentrations ranging from 0.01 µM to 200 µM (Table 5, Figure 6). The IC_{50} was then calculated through concentration-response curves together with NVP as control. Compound **3** was the most active whereas compounds **12**, **15** and **20** were less active. As depicted in Figure 6, the most active compound **3** exhibited an inhibitory activity comparable to that of the commercial compound, having an IC_{50} of 0.63 µM (Table 5), only slighlty higher that the IC_{50} calculated for NVP (IC_{50} = 0.13 µM, Table 5). This indicated that compound **3** has high affinity and inhibitory potency towards RT enzyme and that it could be a promising therapeutic agent for further development. Conversely, compounds **12**, **15** and **20** shared IC_{50} values in the micromolar range. As evidenced by the confidence intervals observed, the estimation of IC_{50} values of these compounds (**12**, **15** and **20,** Table 5) was poor. This was due to their low solubility which limited the evaluation of the inhibitory activity at high concentrations, thus being unable to reach higher inhibition percentage values for these compounds. Moreover, IC_{50} of compound **8** could not be determined as inhibition percentages greater than 50 % could not reached at maximal solubility.

As can be inferred from Tables 2 and 4, there isn't a strong correlation between the predicted pIC_{50} values and the actual inhibitory data. These differences are probably due to the use of heterogeneous sources of biological data for the construction of the computational model. However, the main purpose of this work was to build a selection criteria in order to roughly estimate the inhibitory capabilities of the different compounds and, in this way, as a guide to direct their synthesis. The use of this virtual screening protocol resulted in the preparation of twenty-five quinoxaline derivatives with RT inhibitory activity from a library composing more than 45000 molecules, among which, one of them showed high affinity and inhibitory potency towards this enzyme.

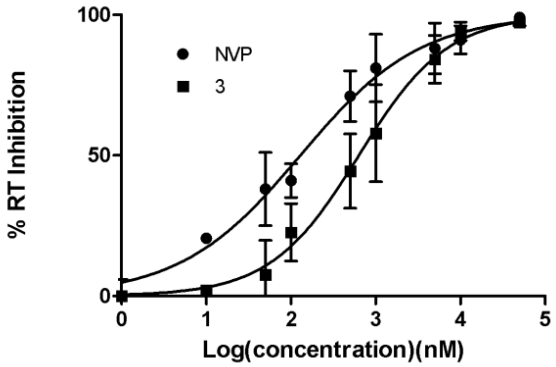

Figure 6. Inhibition of RT activity (IC_{50}) of compound **3** and **NVP**. IC_{50} values were calculated according to the equation for sigmoidal concentration-response using Prism 6.0 (GraphPad Software, San Diego, USA).

Table 5. IC_{50} of **NVP** and compounds **3**,**12, 15** and **20**.

Comp. #	IC_{50} (μM)[a]
NVP	0,13 (0,09-0,17)
3	0,63 (0,53-0,76)
12	64 (38-103)
15	67 (54-87)
20	23 (21-25)

[a] IC_{50} values were determined by measuring fluorescene following exposure to different concentrations of the compounds. IC_{50} values were calculated according to the equation for sigmoidal concentration-response using Prism 6.0 (GraphPad Software, San Diego, USA). Data represent the mean of two independent experiments; the 95% confidence interval is given in parentheses.

It is known that NVP has a low genetic barrier for resistance and that its efficacy is extremely susceptible to mutations in the non-nucleoside inhibitor binding pocket of RT. Particularly, K103N mutation is among the most prevalent mutation in RT and it is associated with resistance to this antiretroviral drug. For this reason, the most potent RT inhibitors in this study, compounds **3**, **12**, **15** and **20**, were tested in HIV-RT enzyme assays using the K103N mutant. To roughly estimate the inhibitors potency towards the mutant enzyme, a single concentration of 50 μM was evaluated for these compounds, and their efficacy was compared against that of the wild-type RT.

Table 6. Percentage K103N RT inhibition by NVP and compounds **3**, **12**, **15** and **20**.

Comp. #	K103N RT inhibition (%)[a]	Fold change[b]
NVP	50 ± 7	2
3	47 ± 7	2

12	13 ± 1	5
15	20 ± 7	3
20	5 ± 1	16

[a] Percentage of K103N inhibition were determined at 50 µM concentration. [b] Fold change was approximate by comparing the percentage of inhibition of the K103N mutant at a concentration of inhibitor of 50 µM versus the percentage of inhibition of the wild-type RT at the same concentration of the inhibitors.

The inhibitory efficacy of the evaluated quinoxaline derivatives shows a 2–16 fold reduction in efficacy when tested against the K103N mutant (Table 6). The effect of the mutation is more pronounced for compound **20** where there is a 16-fold reduction in efficacy compared to wild-type RT. The assay shows that compound **3** is the most potent of the four towards the K103N mutant with an inhibitory behavior close to that of NVP at the single concentration evaluated. Because of the low inhibitory potency of all of the compounds evaluated towards the mutant enzyme, IC_{50} values were not determined.

2.4 Cell toxicity and antiviral activity

The anti-HIV activity and cell toxicity of the synthesized quinoxaline compounds that had showed the highest *in-vitro* RT inhibitory capabilities (**3**, **8**, **12** and **20**, Figure 3) was finally evaluated in cell cultures. Thus, anti-HIV activity (EC_{50}), cytoxocity (CC_{50}) and selectivity index (SI) were determined as described in the experimental section using NVP as reference.

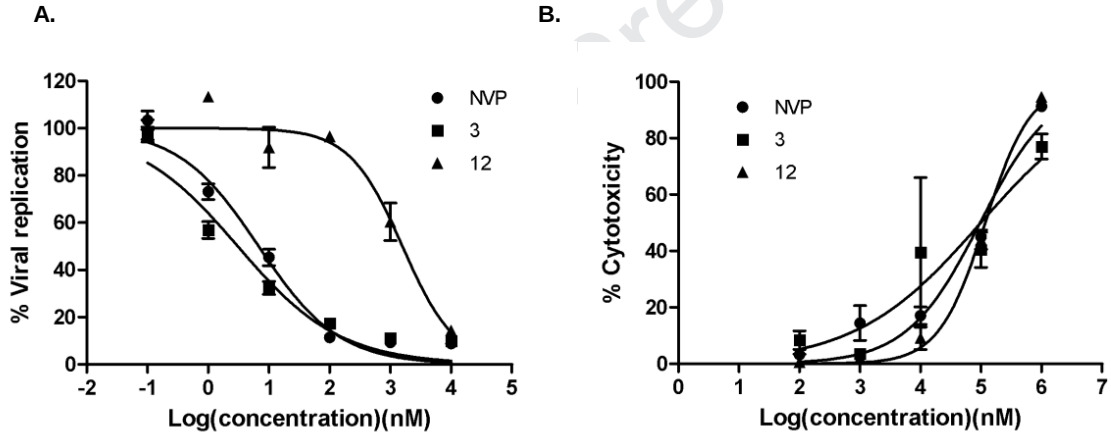

Figure 7. A. % Viral replication and B. Cell viability versus concentration of **NVP** and compounds **3** and **12**.

Table 7. EC_{50}, CC_{50} and SI of **NVP** and compounds **3**, **8**, **12** and **20**.

Compd. #	EC_{50} (nM)[a]	CC_{50} (nM)[b]	SI
NVP	6.7 (4.0-11.3)	96171 (154165-170754)	14353
3	3.1 (1.5-6,2)	98576 (25435-382061)	31798
8	> 10000	262001 (180020-343981)	nc[c]
12	1576 (931-2667)	116818 (94390-144575)	74
20	> 10000	133520 (72634-194405)	nc[c]

*[a] EC50 values were determined by measuring the reduction of syncytia formation following exposure to different concentrations of the compounds in MT2 cells. [b] CC50 values were assessed by Trypan Blue exclusion assays. *[c] not calculated. CC_{50}, EC_{50} values were calculated according to the equation for sigmoidal concentration-response using Prism

6.0 (GraphPad Software, San Diego, USA). Data represent the mean of two independent experiments; the 95% confidence interval is given in parentheses.

To evaluate the effect of the quinoxaline derivatives on viral replication, infected MT2 cells were treated with the different compounds from 0.001 μM to 10 μM and incubated for 4 days at 37℃. In each case, the reduction in the production of p24 antigen was correlated with the reduction in the formation of syncytia. The cell assays indicate a similar inhibitory activity for NVP and compound **3** with an EC_{50} of 6.7 nM and 3.1 nM, respectively (Figure 7, Table 7). Compound **12** also showed good inhibitory properties (EC_{50} of 1576 nM, Table 7) whereas compounds **8** and **20** were not effective as anti-HIV agents (Table 7).

To confirm that the antiviral activity observed with the evaluated compounds at the cellular level was not due to the cellular toxicity associated with their use, the cytotoxicity at different concentrations of the inhibitors was thereof evaluated. In these experiments, uninfected MT2 cells were treated with compounds from 0.01 μM to 1000 μM and were also incubated at 37 ℃ for 4 days. Cell viability was measured for each concentration. All of the evaluated compounds were well tolerated, with CC_{50} at approximately 100-200 μM. Both active compounds (**3** and **12**, Figure 3) showed high selectivity as it is shown by the SI (Table 7).

As shown in Table 7, compound **3** has higher EC_{50} and SI than commercial NVP, with an inhibitory potency in the nanomolar range. Thus, this molecule may be considered a promising lead compound and further studies should be performed to complete the path from lead to clinical drug candidate. Compound **12** also shows good anti-HIV properties in infected cells and SI (hit compound). A hit-to-lead process will be conducted in order to optimize its inhibitory potency.

3. Conclusion

With the aim to find novel HIV RT inhibitors containing a quinoxaline scaffold, we first carried out the construction of a virtual chemical library based on previously described pharmacophore features. The virtual library screening was performed using two complementary computational tools: molecular docking and 3D-QSAR. Based on these results, twenty-five quinoxaline compounds were selected for synthesis. They were then prepared and evaluated as inhibitors of the recombinant wild-type RT enzyme, and the most promising compounds were also evaluated against the K103N RT mutant. Compound **3** demonstrated potent *in-vitro* enzymatic inhibitory activity towards HIV wild-type RT, only slightly weaker than commercial NVP, currently in used in the clinic. When these compounds were evaluated in HIV infected cells, although the two compounds **3** and **12** showed promising anti-HIV activity, compound **12** was the less active. Overall, compound **3** had similar anti-HIV and cytotoxicity profiles than commercial NVP. Taking into account the findings in this study regarding the structural requirements and biological activity profiles of the tested compounds, further development of **3** (lead compound) and **12** (hit compound) will likely provide novel and more potent RT inhibitors for HIV treatment.

4. Experimental

4.1. General

All reactions were carried out using reagent-grade materials under nitrogen atmosphere. Solvents were reagent-grade or better. Silica gel column chromatography was performed using silica gel (Kieselgel 60, 230-400 mesh, Merck). Thin layer chromatography (TLC) was performed on silica gel plates (Kieselgel 60 F254, Merck) having layer thickness of 0.25 mm. ^{1}H and ^{13}C NMR spectra were recorded on a Bruker 300 MHz NMR using $CDCl_3$ and DMSO-d6 as solvent, and tetramethylsilane (TMS) as internal standard. All the chemical shifts values (d) were recorded in parts per million (ppm) and coupling constants (J) in hertz (Hz). IR spectra were recorded using a Perkin Elmer Spectrum One FT-IR spectrophotometer and are expressed in cm^{-1}. High resolution mass spectra were obtained on Bruker micrOTOF-Q II spectrometer. Microwave-assisted reactions were carried out using an Anton Paar Monowave 300 as microwave reactor, stirring at 500 rpm.

4.2. Procedure for the virtual chemistry library construction and virtual screening protocol

4.2.1 Virtual chemistry library construction

The virtual chemistry library (VCL) was constructed using a script that combines the SMILES strings corresponding to the structural scaffolds and the selected substituents (Table 1) as building blocks. The selection of the scaffolds and substituents was based in previously described structural knowledge, obtained from ligand–protein complexes of related compounds and from the two-dimensional pharmacophore model developed by Wang [13]. Also, non-favorable substituents, such as bulky groups, were also included in the library in order to test the accuracy of the virtual screening method. All the possible combinations of the proposed residues gave rise to a VCL composed by a total of 45804 compounds derived from 1,2,3,4-tetrahydroquinoxalin-2-one (tQXN) and from 1,2-dihydroquinoxalin-2-one (dQNX) as scaffolds. Three-dimensional models were built from the isomeric SMILES notations of the assembled VCL compounds and geometry was optimized using the MMFF94 force field [32] (conjugated gradient, convergence criteria of $1x10^{-6}$ or a maximum of 5000 iterations) with OpenBabel 2.3.2 software [33]. Also, non-polar hydrogens were removed from the ligands and Gasteiger charges were assigned employing OpenBabel 2.3.2 software. These models were further evaluated in the screening step.

4.2.2 Virtual screening protocol

The VCL was screened applying a previously developed virtual screening protocol for the search of NNRTI candidates from a compound collection. Briefly, this protocol consists in a combination of docking and 3D-QSAR methods; the first, as a conformer generator and the latter, for compound activity prediction. Both methods were developed, calibrated and validated using RT crystallographic data together with biological activity values extracted from literature.

Initially, docking experiments were used in order to obtain conformers of VCL compounds for further analysis by 3D-QSAR. The experiments were performed using AutodockVina 1.0 software [34] with the settings previously described [21-22] using the RT structure that was extracted from PDBID: 2B6A using USCF Chimera 1.9 software. Only the conformer corresponding to the best scoring docking pose of

those compounds from the VCL that achieved a $\Delta G_{docking} \leq$ -8.0 Kcal/mol were selected for further 3D-QSAR analysis. E3m, E2u and Dv WHIM descriptors [35] were then calculated using PaDEL 2.21 software [36], and pIC_{50} estimated using the 3D-QSAR model previously developed (equation 1).

4.3. Chemistry

*4.3.1 General method for the preparation of N-(2-nitrophenyl)-amino acids (**ND1**-**8**)*

*A. N-(2-nitrophenyl)- aminoacids methyl esters (**ND1**-**4**):*In a typical reaction, the amino acid methyl ester (10 mmol), the corresponding halonitrobenzene (10 mmol), diisopropylamine (22 mmol) and graphene (10 mg) were dissolved and mixed in 10 ml acetonitrile in the provided reaction glass tube equipped with a screw cap and magnetic agitation. The reaction mixture was irradiated with microwaves (Anton PaarMonowave 300 reactor) at 100 ℃ for around 30-40 min. On cooling, the reaction mixture was concentrated, and purified by silica-gel chromatography (hexane/chloroform1:1) to give oily reddish products.

Methyl [(2-nitrophenyl)amino]acetate (**ND1**)

Amino acid employed: Glycine methyl ester. Reaction time: 35 min. Yield: 90 % (yellow oil). MS (m/z): 210.0, ^{1}H-RMN (300 MHz) δ (ppm) ($CDCl_3$): 3.83 (s; 3H; OCH3), 4.11 (d; J=4.40; 2H; CH2), 6,73 (t; J= 8.07 Hz; 1H; ArH), 6.73 (d; J=8.10 Hz; 1H; ArH), 7.48 (t; J= 8.10 Hz; 1H; ArH), 7.48 (d; J= 8.80 Hz; 1H; ArH), 8.41 (sa; 1H; NH).^{13}C-RMN (75 MHz) δ (ppm) ($CDCl_3$): 44.7 (CH_2), 52.6 (OCH_3), 113.6, 116.3, 127.0, 132.8, 136.3, 144.1, 169.8 (C=O).

Methyl-(2S)-2-[(2-nitrophenyl)amino]propanoate (**ND2**)

Amino acid employed: (S)-Alanine methyl ester. Reaction time: 35 min. Yield: 89 % (yellow oil). MS (m/z): 224.0. ^{1}H-RMN (300 MHz) δ (ppm) ($CDCl_3$): 1.67 (d; J= 6.70 Hz; 3H; CH_3), 3.79 (s; 3H; OCH_3), 4.28-4.36 (m; 1H; CH), 6.27 (sa; 1H; NH); 6.70-6.76 (m; 2H; ArH), 7.42-7.48 (m; 1H; ArH), 8.22 (dd; J= 8.80 Hz, J'= 2.00 Hz ; 1H; ArH), 8.32 (sa; 1H; NH). ^{13}C-RMN (75 MHz) δ (ppm) (DMSO-d6): 18.5 (CH_3), 51.1, 52.5, 113.7, 116.1, 126.9, 132.4, 136.2, 146.8, 173.0 (C=O).

Methyl-(2S)-3-methyl-2-[(2-nitrophenyl)amino]butanoate (**ND3**)

Amino acid employed: (S)-Valine methyl ester. Reaction time: 38 min. Yield: 91 % (orange oil). MS (m/z) = 252.0. ^{1}H-RMN (300 MHz) δ (ppm) ($CDCl_3$): 1.08 (d; J= 6.70 Hz; 3H; CH_3), 1.13 (d; J= 7.10 Hz; 3H; CH_3), 2.26-2.49 (m; 1H; CH), 3.77 (s; 3H; OCH_3), 4.07 (t; J= 8.27 Hz; 1H; CH), 6.72 (m; 2H; ArH); 7.44 (t; J= 7.54Hz; 1H; ArH), 8.21 (d; J= 8.55 Hz; 1H; ArH), 8.40 (d; J= 7.00 Hz; 1H; NH). ^{13}C-RMN (75 MHz) δ (ppm) ($CDCl_3$): 18.5 (CH_3), 19.3 (CH_3), 31.4 (CH), 52.3 (OCH_3), 61.7 (CH), 113.7, 116.2, 127.1, 136.3, 136.4, 144.6, 172.2 (C=O).

Methyl-(2S)- 4-methyl-2-[(2-nitrophenyl)amino]pentanoate (**ND4**)

Amino acid employed: (S)-Leucine methyl ester. Reaction time: 40 min. Yield: 90 % (orange oil). MS (m/z): 266.1. ^{1}H-RMN (300 MHz) δ (ppm) ($CDCl_3$): 0.96 (d; J=5.90 Hz; 3H, CH_3), 1.03 (d; J=5.90 Hz; 3H;

CH_3), 1.78-1.88 (m; 3H; $CHCH_2$), 3.76 (s; 3H; OCH_3), 4.25 (m; 1H; NCH), 6.68-6.78 (m; 2H; ArH), 7.44 (t; J= 7.90 Hz; 1H; ArH), 8.20 (dd; J= 8.42 Hz, J'= 1.35 Hz; 1H; ArH), 8.20 (d; J=8.42 Hz; 1H; NH).^{13}C-RMN (75 MHz) δ (ppm) ($CDCl_3$): 21.9 (CH_3), 22.7 (CH_3), 25.0 (CH_2), 41.7 (CH), 52.5 (OCH_3), 54.5 (CH), 113.6, 116.3, 127.0, 132.7, 136.4, 144.3, 173.2 (C=O).

*B. N-(2-nitrophenyl)- amino acids (**ND5-8**)*: In a typical reaction, the corresponding amino acid (10 mmol), FNB (10 mmol), and graphene (10 mg) were dissolved and mixed in 20 ml of a 20 % K_2CO_3 solution in the provided reaction glass tube equipped with a screw cap and magnetic agitation. The reaction mixture was irradiated with microwaves (Anton Parr Monowave 300 reactor) at 120 ℃ for around 15-20 min. After cooling, 30 ml of water was added to the reaction vessel and the aqueous solution was washed with EtOAc. The aqueous layer was acidified using HCl 5 M and extracted with EtOAc. The organic phase was dried over Na_2SO_4 and concentrated to give yellow/orange solids.

Methyl [(2-nitrophenyl)amino]acetate (**ND5**)

Amino acid employed: Glycine. Reaction time: 16 min. Yield: 90 % (yellow solid). Mp: 192-194° C. MS (m/z): 196.0; ^{1}H-RMN (300 MHz) δ (ppm) (DMSO-d6): 4.17 (sa; 2H; CH_2), 6.73 (t; J= 7.47 Hz; 1H; ArH), 6.91 (d; J= 8.50 Hz; 1H; ArH), 7.54 (t; J= 6.88 Hz; 1H; ArH), 8.09 (d; J= 8.60 Hz; 1H; ArH), 8.37 (sa; 1H; NH); ^{13}C-RMN (75 MHz) δ (ppm) (DMSO-d6): 44.6 (CH_2), 115.4, 116.2, 126.6, 131.8. 137.0, 144.9, 171.5 (C=O).

2-[(2-Nitrophenyl)amino]propanoic acid (**ND6**)

Amino acid employed: (S)-Alanine. Reaction time: 15 min. Yield: 92 % (yellow solid). Mp: 144º C. MS (m/z): 210.0. ^{1}H-RMN (300 MHz) δ (ppm) ($CDCl_3$): 1.66 (d; J= 7.16 Hz; 3H; CH_3), 4.28 (m; 1H; CH),; 6.73 (m; 2H; ArH), 7.45 (t; J= 7.60 Hz; 1H; ArH), 8.19 (d; J=7.90 Hz; 1H; ArH), 8.32 (sa; 1H; NH). ^{13}C-RMN (75 MHz) δ (ppm) ($CDCl_3$): 18.5 (CH_3), 51.2 (CH), 113.8, 116.2, 126.9, 132.4, 136.5, 143.8, 177.5 (C=O).

3-Methyl-2-[(2-nitrophenyl)amino]butanoic acid (**ND7**)

Amino acid employed: (S)-Valine. Reaction time: 18 min. Yield: 88 % (yellow solid). Mp: 83º C. MS (m/z): 238.0. ^{1}H-RMN (300 MHz) δ (ppm) ($CDCl_3$): 1.14 (d; J= 7.34 Hz; 3H; CH_3), 1.17 (d; J= 6.25 Hz; 3H; CH_3), 2.34-2.45 (m, 1H, CH), 4.12 (t; J= 8.27 Hz, 1H, CH), 6.75 (m; 2H; ArH), 7.45 (t; J= 7.70 Hz; 1H; ArH), 8.22 (dd; J= 8.53 Hz, J'= 1.10 Hz; 1H; ArH), 8.41 (d; J=7.54 Hz; 1H; NH), 9.10-10.10 (1H; sa; OH). ^{13}C-RMN (75 MHz) δ (ppm) ($CDCl_3$): 18.2 (CH_3), 19.2 (CH_3), 31.2 (CH), 61.2 (CH), 113.7, 116.4, 127.1 132.8, 136.4, 144.4, 177.8 (C=O).

4-Methyl-2-[(2-nitrophenyl)amino]pentanoic acid (**ND8**)

Amino acid employed: (S)-Leucine. Reaction time: 20 min. Yield: 90 % (orange solid). Mp: decomposes. MS (m/z): 252.1. ^{1}H-RMN (300 MHz) δ (ppm) (DMSO-d6): 0.89 (d; J= 6.56 Hz; 3H; CH_3), 0.97 (d; J= 6.56 Hz; 3H, CH_3), 1.70-1.82 (m, 3H, $CHCH_2$), 4.40 (m; 1H; CH), 6.76 (m, 1H; ArH), 6.98 (d; J= 8.25 Hz; 1H; ArH), 7.57 (m; 1H; ArH), 8.10 (dd; J= 8.55 Hz, J= 1.56 Hz; 1H; ArH), 8.17 (d; J= 7.70 Hz; 1H;

NH).[13]C-RMN (75 MHz) δ (ppm) (DMSO-d6): 22.5 (CH_3); 23.1 (CH_3), 25.1 (CH_2), 40.9 (CH), 54.1 (CH), 115.2, 116.6, 126.8, 132.0, 137.3, 144.6, 174.2 (C=O).

*4.3.2. General method for the preparation of tQNXs from N-(2-nitrophenyl)-aminoacids (**tQNX1-4**)*

In a typical reaction, the corresponding N-(2-nitrophenyl)-amino acid (10 mmol) was dissolved and refluxed in ethanol. $SnCl_2$ (36 mmol) in a 5 M solution of HCl (26 ml) was added to the stirred reaction mixture during 1 h, and the mixture was stirred for an additional 1 h. After cooling, the solvent was partially evaporated, and the concentrated solution was left at 5º C for a period of 12 h. The quinoxaline chlorhydrate product precipitated as a red colored solid. The solid product was washed with cold ethanol, vacuum dried and stored as the chlorhydrate stable salt. For product characterization and subsequent reactions, the solid was dissolved in 10% K_2CO_3 solution and the aqueous solution was extracted with EtOAc. The organic phase was dried over Na_2SO_4 and evaporated. In this way, the free quinoxaline bases were obtained.

3,4-Dihydroquinoxalin-2(1*H*)-one(**tQNX1**)

Starting material: **ND5**. Yield: 90%. Mp: 138-140° C. IR (cm^{-1}): 3371, 3183, 1668, 1602, 1504. MS (m/z): 148.2. [1]H-RMN (300 MHz) δ (ppm) (DMSO-d6): 2.49 (sa; 1H; NH), 3.75 (sa; 2H; CH_2), 6.68-6.71 (m; 1H; ArH), 6.75-6.81 (m; 3H; ArH), 10.33 (sa; 1H; NH).[13]C-RMN (75 MHz) δ (ppm) (DMSO-d6): 46.7 (CH_2), 115.1, 115.4, 119.9, 123.0, 127.5, 132.6, 166.6 (C=O).

(3S)-3-Methyl-3,4-dihydroquinoxalin-2(1*H*)-one (**tQNX2**)

Starting material: **ND6**. Yield: 90%. Mp: 110° C. [α]: +8.30 (c 0.6, $CHCl_3$) IR (cm^{-1}): 3370, 3180, 1680, 1600, 1500. MS (m/z): 162.1. [1]H-RMN (300 MHz) δ (ppm) ($CDCl_3$): 1.49 (d; J= 6.71 Hz; 3H; CH_3); 2.64 (sa; 1H; NH); 4.05 (c; J= 6.80 Hz; 1H; CH); 6.71 (d; J= 7.83 Hz; 1H; ArH), 6.76-6.82 (m; 2H; ArH), 6.86-6.96 (m; 1H; ArH), 8.89 (sa; 1H; NH).[13]C-RMN (75 MHz) δ (ppm) ($CDCl_3$): 17.9 (CH_3), 52.0 (CH), 114.1, 115.5, 119.6, 123.8, 125.5, 133.4, 169.6 (C=O).

(3*S*)-3-(Propan-2-yl)-3,4-dihydroquinoxalin-2(1*H*)-one (**tQNX3**)

Starting material: **ND7**. Yield: 75%.Mp: 98-99° C. [α]: +21.0 (c 0.6, $CHCl_3$). IR (cm^{-1}): 3369, 3188, 1688, 1600, 1501. MS (m/z): 190.1. [1]H-RMN (300 MHz) δ (ppm) ($CDCl_3$): 1.00 (d; J= 6.67 Hz; 3H; CH_3), 1.07 (d; J= 6.90 Hz; 3H; CH_3), 2.20-2.37 (m; 1H; CH), 3.80 (d; J= 5.65 Hz; 1H; NCH), 4.09 (sa; 1H; NH), 6.65-6.80 (m; 3H; ArH), 6.89 (td; J= 7.55 Hz, J'=1.10 Hz; 1H; ArH), 9.52 (sa; 1H; NH).[13]C-RMN (75 MHz) δ (ppm) ($CDCl_3$): 17.5 (CH_3), 19.0 (CH_3), 30.9 (CH), 61.8 (CH), 113.4, 115.5, 118.8, 123.9, 124.9, 133.3, 168.7 (C=O).

3-(2-Methylpropyl)-3,4-dihydroquinoxalin-2(1H)-one (**tQNX4**)

Starting material: **ND8**. Yield: 80 %.Mp: decomposes. [α]: +32.0 (c 0.3, $CHCl_3$). IR (cm^{-1}): 3300, 3100, 1670, 1601, 1501. MS (m/z): 204.4. [1]H-RMN (300 MHz) δ (ppm) ($CDCl_3$): 0.97 (d; J= 6.67 Hz; 3H; CH_3), 1.00 (d; J= 6.67 Hz; 3H; CH_3), 1.60-1.73 (m; 2H; CH_2), 1.75-1.87 (m; 1H; CH), 3.96-4.03 (dd; J=8.70 Hz, J'=5.07; 1H; NCH), 4.10 (sa; 1H; NH), 6.66-6.80 (m; 2H; ArH), 6.82-6.94 (m; 2H; ArH), 9.89 (sa; 1H;

NH). ^{13}C-RMN (75 MHz) δ (ppm) ($CDCl_3$): 21.5 (CH_3), 23.2 (CH_3), 24.2 (CH), 40.3 (CH_2), 54.6 (CH), 114.3, 115.7, 119.4, 123.8, 125.6, 132.9, 170.1 (C=O).

*4.3.3. General method for the preparation of N-acylated tQNXs (**1-16**)*

The **tQNX1**-**4** stored as chlorhydrate salts were converted to their free bases as described above. In a typical acylation reaction, the corresponding acylating agent (1.2 mmol) was added to a solution of **tQNX** (1mmol) in EtAcO (30 ml) and triethylamine (1.2 mmol) and heated to reflux for 1 h. After cooling, 50 ml of a 10 % solution of K_2CO_3 was added and the mixture was stirred for additional 15 min. The solution was left still, and the organic phase was separated. The organic phase was then sequentially washed with HCl 0.5 M, 10 % K_2CO_3 and water, dried with Na_2SO_4 and concentrated. The product was characterized without further purification.

4-Acetyl-3,4-dihydroquinoxalin-2(1*H*)-one (**1**)
Starting material: **tQNX1**. Acylating agent: acetyl chloride. Yield: 90%. Mp: 162-163° C. IR (cm $^{-1}$): 3190, 1702, 1666, 1503. MS (m/z): 190.0. ^{1}H-RMN (300 MHz) δ (ppm) ($CDCl_3$): 2.25 (sa; 4H; CH_3, NH), 4.52 (s; 2H; CH_2), 7.04-7.05 (d; J= 7.80 Hz; 1H; ArH), 7.12 (td; J= 7.80 Hz, J'= 1.20 Hz; 1H; ArH), 7.18-7.28 (m; 2H; ArH), 9.74 (sa; 1H; NH).13C-RMN (75 MHz) δ (ppm) ($CDCl_3$): 22.2 (CH_3), 45.5 (CH_2), 116.9, 123.3, 124.0, 127.0, 127.3, 131.2, 167.7 (C=O), 169.8 (C=O).

4-Benzoyl-3,4-dihydroquinoxalin-2(1*H*)-one(**2**)
Starting material: **tQNX1**. Acylating agent: benzoyl chloride. Yield: 90%. Mp: 207° C. IR (cm $^{-1}$): 3266, 1708, 1666, 1500. MS (m/z): 252.0. ^{1}H-RMN (300 MHz) δ (ppm) ($CDCl_3$): 4.63 (s; 2H; CH2); 6.70 (sa, 1H, ArH); 6.80 (t; J= 7.80 Hz ; 1H; ArH); 7.00 (dd; J= 7.80 Hz, J'= 1.40 Hz; 1H; ArH); 7.11 (td; J= 8.40 Hz; J'=1.50 Hz ; 1H; ArH); 7.30-7.40 (m; 2H; ArH); 7.40-7.50 (m; 3H; ArH); 9.34 (sa; 1H; NH). ^{13}C-RMN (75 MHz) δ (ppm) ($CDCl_3$): 47.7 (CH2), 116.5; 123.0; 124.7; 126.2; 128.4; 128.9; 131.2; 134.1; 141.1; 141.4; 168.6 (C=O); 169.3 (C=O).

4-Propanoyl-3,4-dihydroquinoxalin-2(1*H*)-one(**3**)
Starting material: **tQNX1**. Acylating agent: propanoyl chloride. Yield: 90%. Mp: 162° C. IR (cm $^{-1}$): 3084, 1698, 1650, 1497. MS (m/z): 204.2. ^{1}H-RMN (300 MHz) δ (ppm) ($CDCl_3$): 1.19 (t; J=7.32 Hz; 3H; CH_3), 2.57 (c J=7.32 Hz; 2H; CH_2), 4.53 (s; 2H; NCH_2), 7.02 (d; J= 7.80 Hz; 1H; ArH), 7.11 (m; 1H; ArH), 7.20-7.30 (m; 2H; ArH), 9.46 (sa; 1H; NH). ^{13}C-RMN (75 MHz) δ (ppm) ($CDCl_3$): 9.70 (CH_3), 27.2 (CH_2), 46.2 (NCH_2); 116.8 (para 2 C); 123.3; 124.2; 126.8; 127.1, 169.4 (C=O), 173.3 (C=O).

4-(3-Chloropropanoyl)-3,4-dihydroquinoxalin-2(1*H*)-one(**4**)
Starting material: **tQNX1**. Acylating agent: 3-chloropropanoyl chloride. Yield: 95%. Mp: 143-144° C. IR (cm^{-1}): 3084, 1698, 1651, 1496, 747. MS (m/z): 238.7. ^{1}H-RMN (300 MHz) δ (ppm) ($CDCl_3$): 3.04 (t; J= 6.60 Hz; 2H, CH_2), 3.87 (t J=6,60 Hz; 2H; $ClCH_2$), 4.57 (s; 2H; NCH_2), 7.05 (d; J= 7.60 Hz; 1H; ArH), 7.15 (t; J=7.80; 1H; ArH), 7.20-7.40 (m; 2H; ArH), 9.59 (sa; 1H; NH). ^{13}C-RMN (75 MHz) δ (ppm)

($CDCl_3$): 36.6 (CH_2); 39.8 ($ClCH_2$); 45.9 (NCH_2); 116.9; 123.3; 124.0; 127.0; 127.3; 131.2; 169.3 (C=O); 169.5 (C=O).

4-(Chloroacetyl)-3,4-dihydroquinoxalin-2(1*H*)-one (**5**)

Starting material: **tQNX1**. Acylating agent: chloroacetyl chloride. Yield: 95%. Mp :168-170° C. IR (cm^{-1}): 3140, 1702, 1656, 1497, 759. MS (m/z): 224.6. ^{1}H-RMN (300 MHz) δ (ppm) ($CDCl_3$): 4.27 (s; 2H; CH_2), 4.56 (sa; 2H, CH_2); 7.02 (d; J= 7.80 Hz; 1H; ArH); 7.15 (t; J= 7.80 Hz; 1H; ArH); 7.25-7.48 (m; 2H; ArH); 8,90 (sa; 1H; NH). ^{13}C-RMN (75 MHz) δ (ppm) ($CDCl_3$): 40.6 ($ClCH_2$); 46.6 (CH_2); 116,9; 117.0; 123.8; 126.1; 127.8; 131.2; 165.9 (C=O); 166.6(C=O).

4-(Phenylsulfonyl)-3,4-dihydroquinoxalin-2(1*H*)-one (**6**)

Starting material: **tQNX1**. Acylating agent: benzensulfonyl chloride. Yield: 70%. Mp: 183-185° C. IR (cm^{-1}): 3218, 1702, 1693, 1604, 1492. MS (m/z): 288.1. ^{1}H-RMN (300 MHz) δ (ppm) ($CDCl_3$): 4.35 (sa; 2H; CH_2); 6.71 (dd; J= 7,80 Hz, J'=1,10 Hz; 1H; ArH); 7.18 (td; J= 1.30, J'= 7.80; 1H; ArH); 7.22-7.37 (m; 3H; ArH); 7.42-7.55 (m; 3H; ArH); 7.75 (d; J= 7.80 Hz ; 1H; ArH); 8.56 (sa; 1H; NH). ^{13}C-RMN (75 MHz) δ (ppm) ($CDCl_3$): 49.2 (CH_2); 116.2; 124.0; 124.4; 127.0; 127.7; 128.4; 129.0; 132.1; 133.5; 136.8; 166.3 (C=O).

Propan-2-yl 3-oxo-3,4-dihydroquinoxaline-1(2*H*)-carboxylate (**7**)

Starting material: **tQNX1**. Acylating agent: isopropyl chloroformate. Yield: 80%. Mp: 160-161° C. IR (cm^{-1}): 3200, 1712, 1682, 1504. MS (m/z): 234.3. ^{1}H-RMN (300 MHz) δ (ppm) ($CDCl_3$): 1,34 (d; J= 6.03Hz, 3H, CH_3); 1.36 (d; J=6.03Hz; 3H; CH_3); 4.46 (sa; 2H; NCH_2); 5.09 (m; 1H; CH); 6.93 (m; 1H; ArH); 7.11 (m; 2H; ArH); 7.69 (sa; 1H; ArH); 9,05 (sa; 1H; NH).^{13}C-RMN (75 MHz) δ (ppm) ($CDCl_3$): 22.0 (2 x CH_3); 47.4 (CH_2); 70.8 (CH); 116.2; 123.4; 123.9; 125.4; 126.6; 129.8; 153.1 (NC(=O)O); 168.2 (C=O).

2-Methylpropyl 3-oxo-3,4-dihydroquinoxaline-1(2*H*)-carboxylate (**8**)

Starting material: **tQNX1**. Acylating agent: isobutyl chloroformate. Yield: 95 %. Mp: 142-144° C. IR (cm^{-1}): 3199, 1720, 1692, 1600, 1503. MS (m/z): 248.3 ^{1}H-RMN (300 MHz) δ (ppm) ($CDCl_3$): 0.99 (d; J=6,90 Hz; 6H; CH_3); 2,03 (m; 1H; CH); 4,03 (d; J=6,60 Hz; 2H; CH_2); 4.48 (sa; 2H; NCH_2); 6,94 (d; J=7.50 Hz; 1H; ArH); 7.12 (m; 2H; ArH); 7,67 (sa; 1H; ArH); 9,19 (sa; 1H; NH). ^{13}C-RMN (75 MHz) δ (ppm) (CDCl3): 19.1 (2 x CH_3); 27.9 (CH); 47.5 (N-CH_2); 72.9 (O-CH_2); 116.3; 123.4; 124.0; 125.6; 126.5; 129.8; 153.7 (N-C(O)-O); 168.2 (C=O).

(3*S*)-4-(3-Chloropropanoyl)-3-methyl-3,4-dihydroquinoxalin-2(1*H*)-one (**9**)

Starting material: **tQNX2**. Acylating agent: 3-chloropropanoyl chloride. Yield: 95 %. Mp:155-156° C. IR (cm^{-1}): 3200, 1681, 1657, 1503. MS (m/z): 252.7 ^{1}H-RMN (300 MHz) δ (ppm) ($CDCl_3$): 1.27 (d J=6.57; 3H; CH_3); 2.77-2.97 (m, 1H, ClCH2CHH); 3.09-3.26 (m; 1H; $ClCH_2$CHH); 3.73-3.96 (m; 2H; $ClCH_2$); 5.60 (sa; 1H; NCH); 7.04 (d; J=7.42; 1H; ArH); 7.14 (td; J= 7.50 Hz, J'=1.10 Hz; 1H; ArH); 7.20-7.35 (m; 2H; ArH); 9.51 (sa; 1H; NH).^{13}C-RMN (75 MHz) δ (ppm) ($CDCl_3$): 15.3 (CH_3); 37.0 (CH_2); 39.8 ($ClCH_2$); 51.1

(NCH); 116.7; 123.5; 124.1; 125.1; 127.2; 130.9; 169.0 (C=O); 171.9 (C=O). Anal. calc. for $C_{12}H_{13}ClN_2O_2$: C, 57.04; H, 5.19; N, 11.09. Found: C, 57.00; H, 5.25; N, 11.00.

(S)-2-Chloro-1-(2-methyl-3,4-dihydroquinoxalin-1(2*H*)-yl)ethanone(**10**)

Starting material: **tQNX2**. Acylating agent: chloroacetyl chloride. Yield: 80 %. Mp: 198-200° C. IR (cm^{-1}): 3183, 1692, 1650, 1502, 757. MS (m/z): 238.7. ^{1}H-RMN (300 MHz) δ (ppm) ($CDCl_3$): 1.31 (d; J= 7.32 Hz; 3H; CH_3); 4.19 (d J= 14.30 Hz; 1H; ClCHH); 4.33 (d; J= 14.30 Hz; 1H; ClCHH); 5.52 (sa; 1H; NCH); 7.05 (d; J=7.14; 1H; ArH); 7.17 (t; J= 7.40 Hz; 1H; ArH); 7.22-7.35 (m; 1H; ArH); 7.35-7.47 (m; 1H; ArH); 9.41 (sa; 1H; NH). ^{13}C-RMN (75 MHz) δ (ppm) ($CDCl_3$): 15.2 (CH_3); 41.4 ($ClCH_2$); 52.0 (NCHCO); 116,8; 123.8; 123.9; 127.7; 130.7; 130.9; 165.8 (C=O); 171.3 (C=O). Anal. calc. for $C_{11}H_{11}ClN_2O_2$: C, 55.36; H, 4.65; N, 11.74. Found: C, 55.30; H, 4.68; N, 11.70.

(3S)-3-Methyl-4-propanoyl-3,4-dihydroquinoxalin-2(1H)-one (**11**)

Starting material: **tQNX2**. Acylating agent: propanoyl chloride. Yield: 90 %. Mp: 176-177° C. IR (cm^{-1}): 3183, 1702, 1650, 1500. MS (m/z): 218.3. ^{1}H-RMN (300 MHz) δ (ppm) ($CDCl_3$): 1.20 (t; J= 7.13 Hz; 3H; CH3); 1.26 (d J= 7.22 Hz; 3H; CH_3); 2.38-2.56 (m; 1H, ;CHH); 2.57-2.75 (m; 1H; CHH); 5.59 (sa; 1H; NCHCO); 6.98 (d; J=7.23; 1H; ArH); 7.12 (t; J= 7.61 Hz; 1H; ArH); 7.23 (t J=7.61; 1H; ArH); 7.27-7.34 (m; 1H; ArH); 8.98 (sa; 1H; NH).^{13}C-RMN (75 MHz) δ (ppm) ($CDCl_3$): 15.2 (CH_3); 27.5 (CH_2); 52.0 (NCH); 116,3; 123.3; 124.8; 125.2; 126.6; 130.5; 168.0 (C=O); 173.0 (C=O). Anal. calc. for $C_{12}H_{14}N_2O_2$: C, 66.04; H, 6.47; N, 12.84. Found: C, 66.00; H, 6.49; N, 12.70.

2-Methylpropyl (2*S*)-2-methyl-3-oxo-3,4-dihydroquinoxaline-1(2*H*)-carboxylate(**12**)

Starting material: **tQNX2**. Acylating agent: isobutyl chloroformate. Yield: 90 %. Mp: 165-167° C. IR (cm^{-1}): 3193, 1720, 1681, 1600, 1503. MS (m/z): 262.2. ^{1}H-RMN (300 MHz) δ (ppm) ($CDCl_3$): 0.99 (d; J=6.25Hz; 6H; 2xCH_3); 1.31 (d; J= 7.22 Hz, 3H, CH_3); 1.92-2.14 (m; 1H; CH); 4,05 (ac; 2H; CH_2); 5.23 (ac; J= 6.27 Hz; 1H; NCH); 6,89-6.99 (m; 1H; ArH); 7.03-7.20 (m; 2H; ArH); 7.69 (sa; 1H; ArH); 9.12 (sa; 1H; NH). ^{13}C-RMN (75 MHz) δ (ppm) ($CDCl_3$): 16.0 (CH_3), 19.1 (2 x CH_3); 27.9 (CH); 53.2 (NCH); 72.7 (OCH_2); 115.9; 123.5; 124.3; 124.8; 125.4; 129.1; 153.5 (NC(=O)O); 170.7 (C=O). Anal. calc. for $C_{14}H_{18}N2O_3$: C, 64.10; H, 6.92; N, 10.68. Found: C, 64.00; H, 6.98; N, 10.62.

(3*S*)-4-(Chloroacetyl)-3-(propan-2-yl)-3,4-dihydroquinoxalin-2(1*H*)-one(**13**)

Starting material: **tQNX3**. Acylating agent: Chloroacetyl chloride. Yield: 75 %. Mp: 215-216° C. IR (cm^{-1}): 3190, 1674, 1603, 1503. MS (m/z): 266.7. ^{1}H-RMN (300 MHz) δ (ppm) ($CDCl_3$): 0.91 (sa; 3H; CH_3); 1.09 (d; J= 6.81 Hz; 3H; CH_3); 1.65-1.75 (m; 1H; CH); 4.16 (d; J= 12.32 Hz; 1H; ClCHH); 4.34 (d; J= 12.32 Hz; 1H; ClCHH); 5.09 (m; 1H; NCH); 7.00 (d; J=7.42; 1H; ArH); 6.89 (td; J= 7.80 Hz, J= 1.35 Hz; 1H; ArH); 7.22-7.32 (m; 1H; ArH); 7.35-7.45 (m; 1H; ArH); 8.81 (sa; 1H; NH). ^{13}C-RMN (75 MHz) δ (ppm) ($CDCl_3$): 19.1 (2 x CH_3); 28.5 (CH); 40.4 ($ClCH_2$); 61.1 (NCH); 116,7; 123.6; 123.8; 127.7; 131.0; 131.1; 166.3 (C=O); 169.3 (C=O). Anal. calc. for $C_{13}H_{15}ClN_2O_2$: C, 58.54; H, 5.67; N, 10.50. Found: C, 58.50; H, 5.70; N, 10.48.

(3*S*)-4-(3-Chloropropanoyl)-3-(propan-2-yl)-3,4-dihydroquinoxalin-2(1*H*)-one(**14)**

Starting material: **tQNX3**. Acylating agent: 3-Chloropropionyl chloride. Yield: 80 %. Mp: 179-180° C. IR (cm^{-1}): 3200, 1687, 1657, 1600, 1503, 748. MS (m/z): 280.8. ^{1}H-RMN (300 MHz) δ (ppm) ($CDCl_3$): 0.90 (d; J=6.51; 3H; CH_3); 1.08 (d; J= 6.51 Hz; 3H; CH_3); 1.69 (m; 1H; CH); 2.77-2.86 (m; 1H; $ClCH_2CHH$); 3.19-3.28 (m; 1H; $ClCH_2CHH$); 3.76-3.84 (m; 1H; ClCHH); 3.88-3.97 (m; 1H; ClCHH); 5.14 (d; J=8.05; 1H; NCH); 7.00 (d; J=7.42; 1H; ArH); 6.89 (td J=1.35 Hz, J'= 7.80 Hz; 1H; ArH); 7.22-7.32 (m; 1H; ArH); 7.35-7.45 (m; 1H; ArH); 8.81 (sa; 1H; NH). ^{13}C-RMN (75 MHz) δ (ppm) ($CDCl_3$): 18.9 (2 x CH_3); 28.3 (CH); 36.7 (CH_2); 40.1 ($ClCH_2$); 60.7 (NCH); 116,5; 123.4; 124.9; 125.2; 127.2; 131.2; 169.5 (C=O); 171.7 (C=O). Anal. calc. for $C_{14}H_{17}ClN_2O_2$: C, 59.89; H, 6.10; N, 9.98; Found: C, 59.80; H, 6.15; N, 9.95.

2-Methylpropyl (2*S*)-2-(2-methylpropyl)-3-oxo-3,4-dihydroquinoxaline-1(2*H*)-carboxylate(**15**)

Starting material: **tQNX4**. Acylating agent: isobutyl chloroformate. Yield: 85 %. Mp: 149-151° C. IR (cm^{-1}): 3185, 1704, 1685, 1603, 1503. MS (m/z): 304.4. ^{1}H-RMN (300 MHz) δ (ppm) ($CDCl_3$): 0.92 (d; J= 6.73 Hz; 3H; CH_3); 0.94-1.01 (sa; 6H; 2xCH_3); 1.02(d; J= 6.73 Hz; 3H; CH_3); 1.36-1.46 (m; 2H; CH_2); 1.65-1.77 (m; 1H; CH); 2.02 (sa; 1H; CH); 3.90-4.20 (sa; 2H; OCH_2); 5.19 (ac;1H; NCH); 6.92 (d; J=7.41 Hz; 1H; ArH); 7.11 (t; J=7.16 Hz; 1H; ArH); 7.16 (t; J=7.41 Hz; 1H; ArH); 7.60 (sa; 1H; ArH); 8.80 (sa; 1H; NH).^{13}C-RMN (75 MHz) δ (ppm) ($CDCl_3$): 19.1 (CH_3); 19.2 (CH_3); 21.9 (CH_3); 22.9 (CH_3); 24.4 (CH); 27.9 (CH); 38.5 (CH_2); 55.7 (NCH); 72.9 (OCH_2); 115.8; 123.8, 125.7; 126.1; 129.8; 154.1 (C=O), 171.5 (C=O). Anal. calc. for $C_{17}H_{24}N_2O_3$: C, 67.08; H, 7.95; N, 9.20. Found: C, 67.00; H, 7.99; N, 9.18.

(3*S*)-4-(3-Chloropropanoyl)-3-(2-methylpropyl)-3,4-dihydroquinoxalin-2(1*H*)-one(**16)**

Starting material: **tQNX4**. Acylating agent: 3-Chloropropionyl chloride. Yield: 85 %. Mp: 150-151° C. IR (cm^{-1}): 3203, 1681, 1651, 1502, 746. MS (m/z): 294.7. ^{1}H-RMN (300 MHz) δ (ppm) ($DCCl_3$): 0.89 (d; J= 6.19 Hz; 3H; CH_3); 1.03 (d; J= 6.19 Hz; 3H; CH_3); 1.29-1.37 (m; 1H; CHH); 1.38-1.46 (m; 1H; CHH); 1.57 (m; 1H; CH); 2.81 (dt; J=16.1 Hz, J'=6.59 Hz; 1H; CHH); 3.19 (dt; J=15.9 Hz, J'=6.60 Hz; 1H; CHH); 3.77-3.85 (m; 1H; ClCHH); 3.87-3.94 (m; 1H; ClCHH); 5.57 (dd; J=11.3 Hz, J'=4.23 Hz; 1H; NCH); 7.01 (d; J=7.29 Hz; 1H; ArH); 7.15 (td; J=7.60 Hz, J'=1.02 Hz; 1H; ArH); 7.25-7.30 (m; 2H; ArH); 8.99 (sa; 1H; NH). ^{13}C-RMN (75 MHz) δ (ppm) ($CDCl_3$): 21.7 (CH_3); 23.0 (CH_3); 24.6 (CH); 36.9 (CH2); 37.6 (CH_2); 39.9 (CH_2); 53.9 (NCH); 116.6; 123.5; 124.4; 125.4; 127.5; 131.3; 169.5 (C=O), 171.5 (C=O). Anal. calc. For $C_{15}H_{19}ClN_2O_2$: C, 61.12; H, 6.50; N, 9.50;. Found: C, 61.10; H, 6.52; N, 9.48.

*4.3.4. General method for the preparation of dQNXs**17-18-21-22***

In a typical reaction, o-phenyldiamine (10 mmol) and the corresponding dicarbonylic compound (10 mmol) were dissolved in ethanol (5 ml) in a reaction glass tube equipped with a screw cap and magnetic agitation. The reaction mixture was irradiated with microwaves (Anton Parr Monowave 300 reactor) at 30 W for around 5-13 min. After cooling, 10 ml of ethanol was added to the reaction vessel. The product was recrystallized from ethanol, precipitating as a white solid.

3-Methylquinoxalin-2(1*H*)-one(**17**)

Dicarbonyl compound: pyruvic acid. Reaction time: 8.5 min. Yield: 98 %. Mp: 243-245°. IR (cm^{-1}): 3045, 1670, 1640. MS (m/z): 160.2. ^{1}H-RMN (300 MHz) δ (ppm) (DMSO-d6): 2,39 (s; 3H; CH_3); 7.22-7.35 (sa; 2H; ArH); 7.41-7.54 (sa; 1H; ArH); 7.64-7.74 (sa; 1H; ArH); 12,33 (sa; 1H; NH). ^{13}C-RMN (75 MHz) δ (ppm) ($CDCl_3$): 21.0 (CH_3); 115.7; 123.5; 128.3; 129.8; 132.1; 132,3; 155.4 (C=N); 159.9 (C=N).

1,4-Dihydroquinoxaline-2,3-dione (**18**)

Dicarbonyl compound: oxalic acid. Reaction time: 6 min. Yield: 90 %. Mp >320° C. IR (cm^{-1}): 3043, 1681, 1613, 1500. MS (m/z): 162.1. ^{1}H-RMN (300 MHz) δ (ppm) (DMSO-d_6): 7.02-7.20 (m; 4H; ArH); 11.93 (s.a.; 2H; NH). ^{13}C-RMN (75 MHz) δ (ppm) (DMSO-d_6): 115.6; 123.5; 126.0; 155.7 (C=N).

3-Benzylquinoxalin-2(1*H*)-one(**21**)

Dicarbonyl compound: Phenylpyruvic acid. Reaction time: 13 min. Yield: 95 %. Mp: 198 - 200° C. IR (cm^{-1}): 3061, 1655, 1597, 1500. MS (m/z): 236.2. ^{1}H-RMN (300 MHz) δ (ppm) (DMSO-d_6): 4.13 (s; 2H; CH_2); 7.16-7.38 (m; 7H; ArH); 7.49 (t; J=7.24 Hz; 1H; ArH); 7.73 (d; J= 8.11 Hz; 1H; ArH); 12,39 (s.a.; 1H; NH). ^{13}C-RMN (75 MHz) δ (ppm) (DMSO-d_6): 39.9 (CH_2); 115.7; 123.6; 126.7; 128.7; 128.8; 129.6; 130.2; 132.1; 132.4; 137.9; 155.5 (C=N); 160.8 (C=N).

3-(3-Oxo-3,4-dihydroquinoxalin-2-yl)propanoicacid (**22**)

Dicarbonyl compound: alpha-ketoglutaric acid. Reaction time: 5 min. Yield: 98 %. Mp: 256 - 258° C. IR (cm^{-1}): 3435, 3102, 1730, 1666, 1608, 1502. MS (m/z): 218.1^{1}H-RMN (300 MHz) δ (ppm) (DMSO-d_6): 2.72 (t; J=6.30 Hz; 2H; CH_2); 3.02 (t; J=6.30 Hz; 2H; CH_2); 7.21-7.35 (m; 2H; ArH); 7.46 (t; J= 7.65 Hz; 1H; ArH), 7.69 (d; J= 8.06, 1H, ArH), 12.10 (s.a.; 1H; OH); 12.30 (s.a.; 1H; NH). ^{13}C-RMN (75 MHz) δ (ppm) (DMSO-d_6): 28.1; 30.4; 115.7; 123.5; 128.5; 129.9; 131.9, 132.1; 155.0 (C=N); 160.7 (C=O); 174.4 (COOH).

*4.3.5. General method for the preparation of dQNXs **19-20***

Typically, 0.5 ml of H_2O_2 (100 vol) were added to a 10% K_2CO_3 solution (50 ml) of the corresponding tetrahydroquinixalinic derivatives (10 mmol). The reaction mixture was heated to reflux for 1 h. After cooling, the reaction mixture was extracted with EtAcO. The organic phase was dried over Na_2SO_4 and concentrated. The residue was recrystallized from ethanol precipitating as a white solid.

3-(Propan-2-yl)quinoxalin-2(1*H*)-one(**19**)

Yield: 70%. Mp: 190° C.IR (cm^{-1}): 3120, 1660, 1490. MS (m/z): 188.1. ^{1}H-RMN (300 MHz) δ (ppm) (DMSO-d6): 1.39 (d; J= 6.83 Hz; 6H, CH_3); 3.60-3.75 (m, 1H, CH); 7.30-7.40 (m; 2H; ArH); 7.50 (t; J= 7.94 Hz; 1H; ArH); 7.87 (d; J= 7.94 Hz; 1H; ArH); 11.78 (s.a.; 1H; NH).^{13}C-RMN (75 MHz) δ (ppm) (DMSO-d6): 23.2 (2 x CH_3); 30.7 (CH); 115.3; 124.0; 128.9; 129.5; 130.8; 132.9; 156.0 (C=N); 165.6 (C=O).

3-(2-Methylpropyl)quinoxalin-2(1*H*)-one(**20**)

Yield: 70%. Mp: 184-185° C. IR (cm^{-1}): 3308, 1661, 1600, 1556. MS (m/z): 202.3. ^{1}H-RMN (300 MHz) δ (ppm) (DMSO-d6): 0.94 (d; J= 6.79 Hz; 6H; CH_3); 2.19-2.31 (m; 1H; CH); 2.67 (d; J= 6.40 Hz; 2H; CH_2); 7.23-7.33 (m; 2H; ArH); 7.48 (t; J= 7.56 Hz; 1H; ArH); 7.73 (d; J= 8.31 Hz; 1H; ArH); 12,32 (s.a.; 1H; NH). ^{13}C-RMN (75 MHz) δ (ppm) (DMSO-d6): 23.0 (2 x CH_3); 26.6 (CH); 42.0 (CH_2); 115.7; 123.5; 128.6; 129.9; 132.1; 132.2; 155.3 (C=N); 161.7 (C=O).

*4.3.6. General method for the preparation of dQNXs (**23**-**25**) from compound **22.***

Methanesulfonic acid supported on Al_2O_3 (AMA 2:3) was prepared mixing Al_2O_3 (3 mol), previously activated in an oven at 150 ℃ for 72 h, with CH_3SO_3H (2 mol) in a mortar until homogeneity.

In a typical reaction, AMA 2:3 (10 mmol), the corresponding carboxylic acid (1 mmol) and the alcohol (2 ml) were mixed in the provided reaction glass tube equipped with a screw cap and magnetic agitation until a wet mixture was achieved. The reaction mixture was irradiated with microwaves (Anton Parr Monowave 300 reactor) at 120 ℃ for 10-25 min. On cooling, the mixture was diluted with DCM (41 mL), and filtered over celite. Then the filtrate was washed with Na_2CO_3 (ss) and water. The organic layer was dried over Na_2SO_4, filtered, and concentrated under reduced pressure to give the ester.

Methyl 3-(3-oxo-3,4-dihydroquinoxalin-2-yl)propanoate (**23**)

Alcohol: Methanol. Reaction time: 10 min. Yield: 95%. Mp: 208-209° C. IR (cm^{-1}): 1730, 1655, 1615, 1510, 1490, 1565. MS (m/z): 232.3. ^{1}H-RMN (300 MHz) δ (ppm) (DMSO-d6): 2.79 (t; J=7.01 Hz; 2H; CH_2); 3.06 (t; J=6.83 Hz; 2H; CH_2); 3.60 (s; 3H; OCH_3); 7.23-7.33 (m; 2H; ArH); 7.48 (t; J= 7.99 Hz; 1H; ArH), 7.68 (d; J= 8.40; 1H; ArH), 12.36 (s.a.; 1H; NH).^{13}C-RMN (75 MHz) δ (ppm) (DMSO-d6): 28.0 (CH_2); 29.8 (CH_2); 51.8 (OCH_3); 115.7; 123.6; 128.6; 130.0; 131.9; 132.2; 155.0 (C=N); 160.4 (C=O); 173.4 (CO).

Ethyl 3-(3-oxo-3,4-dihydroquinoxalin-2-yl)propanoate (**24**)

Alcohol: Ethanol. Reaction time: 20 min.Yield: 95%. Mp: 186-188° C. IR (cm^{-1}): 1727, 1677, 1668, 1617, 1510, 1490, 1572. MS (m/z): 246.3. ^{1}H-RMN (300 MHz) δ (ppm) (DMSO-d6): 1.17 (t; J=7.01 Hz; 2H; CH_3); 2.77 (t; J=6.95 Hz; 2H; CH_2); 3.05 (t; J=6.95 Hz; 2H; CH_2); 4.06 (c; J= 7.25 Hz; 2H, OCH_2); 7.23-7.33 (m; 2H; ArH); 7.43-7.51 (t; J= 7.74 Hz; 1H; ArH), 7.67 (d; J= 7.55 Hz; 1H; ArH), 12.36 (s.a.; 1H; NH). ^{13}C-RMN (75 MHz) δ (ppm) (DMSO-d6): 14.6 (CH_3); 28.1 (CH_2); 30.1 (CH_2); 60.2 (OCH_2); 115.7; 123.6; 128.5; 130.0; 131.9; 132.2; 155.0 (C=N); 160.4 (C=O); 172.8 (CO).

Propan-2-yl 3-(3-oxo-3,4-dihydroquinoxalin-2-yl)propanoate (**25**)

Alcohol: Isopropyl alcohol. Reaction time: 25 min.Yield: 90%. Mp: 178-179° C. IR (cm^{-1}): 1719, 1666, 1651, 1562, 1427, 1186. MS (m/z): 260.2. ^{1}H-RMN (300 MHz) δ (ppm) (DMSO-d6): 1.17 (d; J=7.01 Hz; 3H; CH_3); 1.18 (d; J=7.01 Hz; 3H; CH_3); 2.73 (t; J=6.80 Hz; 2H; CH_2); 3.04 (t; J=6.80 Hz; 2H; CH_2); 4.88 (m; 1H; CH); 7.23-7.33 (m; 2H; ArH); 7.48 (t; J= 7.74 Hz; 1H; ArH), 7.65 (d; J= 7.14 Hz; 1H, ArH), 12.35 (s.a.; 1H; NH). ^{13}C-RMN (75 MHz) δ (ppm) (DMSO-d6): 22.1 (2 x CH_3); 28.2 (CH_2); 30.4 (CH_2); 67.4 (OCH); 115.7; 123.6; 128.4; 129.9; 131.9, 132.1; 155.0 (C=N); 160.5 (C=O); 172.3 (CO).

4.4. Biology

4.4.1. HIV-1 RT inhibition enzyme assay

The p66/p51 HIV-1 wild-type and K103N reverse transcriptase heterodimer overexpression and purification were carried out by means of the plasmids gently donated by Dr. Stephen Hughes according to the procedures previously described [37]. The RT recombinant enzyme is from subtype B HIV, strain BH10 (Genebank HIVBH102). RT activity was measured using the commercial kit EnzChek® Reverse Transcriptase Assay Kit (Invitrogen Co., USA) according to the manufacturer's instructions, with minor modifications. Briefly, 2 µl of a solution of the different inhibitors were incubated with 10 µl of the recombinant RT enzyme (approximately 50 nM) in reaction buffer in a 96-well solid black plate for fluorescence reading. After 2 min, the previously incubated templates poly (A) and oligo-dT were added. The reaction mixture was then incubated for 2 h at room temperature. The resulting DNA heteroduplexes generated in each well were then detected and quantitatively measured using the PicoGreen reagent (173 µl) provided in the kit using a FlexStation 3 microplate reader (Molecular Devices Inc., San Jose, CA, United States).at an excitation wavelength of 480 nm and an emission wavelength of 520 nm. Nevirapine was used as positive control. All experiments were performed in triplicate wells for each condition and repeated at least twice. The results are expressed as percentage (%) of inhibition, comparing the activity of the enzyme incubated with the inhibitor with the activity without any additives. The half maximal inhibitory concentration (IC_{50}) was determined by concentration-responses curves varying the amount of inhibitor in each well. The values were calculated according to the equation for sigmoidal concentration-response using Prism 6.0 (GraphPad Software, San Diego, USA).

4.4.2. Cells based assays

Cells: MT2 cell line was cultured in RPMI-1640 medium (HyClone USA) supplemented with 10% fetal bovine serum (Sigma-Aldrich USA), 2 mML-glutamine (Sigma-Aldrich), 100 U/ml penicillin (Sigma-Aldrich), 100 mg/ml streptomycin (Sigma-Aldrich), and 10 mM HEPES (Sigma-Aldrich).

Virus: Viral stock HTLV-IIIB (laboratory strain of the HIV-1 virus provided by the McGill AIDS Center, Montreal, Canada.) Produced from chronically infected H9 cells and propagated in MT2 cells. Title of viral stock used: 1.58 x 10^6 $TCID_{50}$/ml.

4.4.2.1 Cytotoxicity tests: The toxicity of the compounds was tested by performing 10-fold serial dilutions of both compounds, from 0.01 µM to 1000 µM, and subsequently incubated with the MT2 cells without infecting. The toxic effect was evaluated at 4 days by Trypan Blue dye and subsequent counting of viable cells in Neubauer chamber. All experiments were performed in duplicate for each condition and repeated at least twice.

4.4.2.2. Inhibition assays of viral activity: First, MT2 cells were incubated with a 1/5 dilution of de viral stock in complete culture medium (at a concentration of 1 M cell / ml virus dilution) for 2 hours at 37 °C. The cells were washed and resuspended in fresh medium. Infected cells were incubated with the 10-fold serial dilutions of the compounds, from 0.001 µM to 10 µM. The supernatants were collected after 4

days. The production of p24 antigen was evaluated by Elisa (Fujirebio Japan). All experiments were performed in duplicate for each condition and repeated at least twice.

Conflicts of interest

The authors declare no conflict of interest.

Acknowledgements

This work was financially supported by AgenciaNacional de Promoción Científica y Tecnológica, Universidad de Buenos Aires and Consejo Nacional de Investigaciones Científicas y Tecnológicas (Argentina) grants. Special thanks to Emiliano Barrionuevo and Gabriel Jasinsky for their assistance on this publication.

References

1. http://www.unaids.org/en/resources/fact-sheet

2. Fernández-Montero, J.V., Vispo, E., Soriano, V., (2014) Emerging antiretroviral drugs, *Expert Opinion on Pharmacotherapy*, 15(2): 211-219, DOI:10.1517/14656566.2014.863277

3. https://www.fda.gov/forpatients/illness/hivaids/treatment/ucm118915.htm

4. Usach, I., Melis, V., Peris, J. (2013) Non-nucleoside reverse transcriptase inhibitors: a review on pharmacokinetics, pharmacodynamics, safety and tolerability. *Journal of the International AIDS Society*, 16: 18567,DOI:10.7448/IAS.16.1.18567

5. Shi, L., Hu, W., Wu, J., Zhou, H., Zhou, H., Li, X. (2018) Quinoxalinone as a Privileged Platform in Drug Development, *Mini-Reviews in Medicinal Chemistry*, 18: 392-413, DOI: 10.2174/1389557517666171101111134

6. Husain, A., Madhesia, D., (2011) Recent advances in pharmacological activities of quinoxaline derivatives*, Journal of Pharmacy Research*, 4 (3): 924-929

7. Kleim, J.P., Bender, R, Kirsch, R., (1995) Preclinical evaluation of HBY 097, a new nonnucleoside reverse transcriptase inhibitor of human immunodeficiency virus type 1 replication, *Journal of Antimicrobial.* Chemotherapy, 39: 2253-2257, DOI:10.1128/aac.39.10.2253

8. Patel, M., McHugh, R.J, Cordova, B.C., Klabe, R.M., Erickson-Viitanen, S., Trainor, G.L., Rodgers, J.D., (2000) Synthesis and evaluation of quinoxalinones as HIV-1 reverse transcriptase inhibitors, *Bioorganic & Medicinal Chemistry Letters*, 10 (15): 1729-1731, DOI:10.1016/s0960-894x(00)00321-8

9. Balzarini, J., Karlsson, A., Meichsner, C., Paessens, A., Riess, G., DeClercq, E., Kleim, J.P., (1994) Resistance pattern of human immunodeficiency virus type 1 reverse transcriptase to quinoxaline S-2720, *Journal of Virology*, 68 (12): 7986-7992.

10. Sheran, M., (2005) The Nonnucleoside Reverse Transcriptase Inhibitors Efavirenz and Nevirapine in the Treatment of HIV, *HIV Clinical Trials*, 6(3):158-168, DOI:10.1310/4KC0-56TM-VLBF-78BN

11. Althaus, I.W., Gonzales, A.J., Chou, J.J., Romero, D.L., Deibel, M.R., Chou, K.C., Kezdy, F.J., Resnick, L., Busso, M.E., So, A.G., (1993) The quinoline U-78036 is a potent inhibitor of HIV-1 reverse transcriptase, Journal of*. Biological Chemistry*, 268: 14875-14880.

12. Rubinek, T., McMahon, J. B., Hizi, A. (1994) Inhibition of reverse transcriptase of human immunodeficiency virus type 1 and chimeric enzymes of human immune deficiency viruses types 1 and 2 by two novel non-nucleoside inhibitors, *FEBS Letters*, 350, DOI: 10.1016/0014-5793(94)00793-413.

13. Wang, J., Kang, X., Kuntz, I.D., Kollman, P.A., (2005) Hierarchical Database Screenings for HIV-1 Reverse Transcriptase Using a Pharmacophore Model, Rigid Docking, Solvation Docking, and MM−PB/SA, *Journal of Medicinal Chemistry*,*48*(7): 2432-2444, DOI: 10.1021/jm049606e

14. Jorgensen, W.L., Ruiz-Caro, J., Tirado-Rives, J., Basavapathruni, A., Anderson, K.S., Hamilton, A.D., (2006) Computer-aided design of non-nucleoside inhibitors of HIV-1 reverse transcriptase, *Bioorganic & Medicinal Chemistry Letters*, 16(3): 663-667, DOI: 10.1016/j.bmcl.2005.10.038

15. Jorgensen, W.L., (2016) Computer-aided discovery of anti-HIV agents, *Bioorganic & Medicinal Chemistry*, 24 (20): 4768-4778, DOI: 10.1016/j.bmc.2016.07.039

16. Paneth, A., Płonka, W., Paneth, P., (2017) What do docking and QSAR tell us about the design of HIV-1 reverse transcriptase nonnucleoside inhibitors?, *Journal of Molecular Modeling.*, 23: 317. DOI: 10.1007/s00894-017-3489-311.

17. Carta, A., Pricl, S., Piras, S., Fermeglia, M., La Colla, P., Loddo, R., (2009) Activity and molecular modeling of a new small molecule active against NNRTI-resistant HIV-1 mutants, *European Journal of Medicinal Chemistry*, 44 (12): 5117-5122, DOI:10.1016/j.ejmech.2009.08.012

18. Ragno, R., Frasca, S., Manetti, F., Brizzi, A., Massa, S., (2005) Reverse Transcriptase Inhibition: Inclusion of Ligand-Induced Fit by Cross-Docking Studies, *Journal of Medicinal Chemistry*,*48*(1): 200-212, DOI: 10.1021/jm049392

19. Poongavanam, V., Namasivayam, V., Vanangamudi, M., Al Shamaileh, H., Veedu, R. N., Kihlberg, J. and Murugan, N. A. (2018) Integrative approaches in HIV-1 non-nucleoside reverse transcriptase inhibitor design, *WIREs Computational. Molecular Science*, 8: e1328,DOI:10.1002/wcms.1328

20. Patel, S.B., Patel, B.D., Pannecouque, C., Bhatt, H.G., (2016) Design, synthesis and anti-HIV activity of novel quinoxaline derivatives, *European Journal of Medicinal Chemistry*, 117: 230-240, DOI:10.1016/j.ejmech.2016.04.019

21. Fabian, L., Gómez, N., Jasinski G., Estrin, D., Moglioni, A., (2014) NNRTI HIV Chemotherapeutics: Docking and 3D-QSAR as complementary strategies in virtual screening of quinoxaline analogues library, *European Journal Pharmaceutical Sciences,* 50 (1), E1-E138

22. Lucas, F., Emanuel *Diseño y síntesis de análogos quinoxalínicos con potencial actividad quimioterápica* (Tesis doctoral, May 5th, 2015). Universidad de Buenos Aires. Facultad de Farmacia y Bioquímica.

Link:http://repositoriouba.sisbi.uba.ar/gsdl/cgibin/library.cgi?a=d&c=posgrauba&cl=CL1&d=HWA_1139

23 Fabian, L., Gómez, M., Caturelli Kuran, J.A., Moltrasio, G., Moglioni, A., (2014) Efficient Microwave-Assisted Esterification Reaction Employing Methanesulfonic Acid Supported on Alumina as Catalyst, *Synthetic Communications, 44(16): 2386-2392,* DOI:10.1080/00397911.2013.875210

24. TenBrink, R.E., Im, W., Sethy, V.H., Tang, A.H., Carter, D.B., (1994**)** Antagonist, Partial Agonist, and Full Agonist Imidazo[1,5-a]quinoxaline Amides and Carbamates Acting through the GABAA/Benzodiazepine Receptor, *Journal of Medicinal Chemistry ,37*(6): 758-768, DOI: 10.1021/jm00032a008

25. Garg, B., Bisht, T., Ling, Y. C., (2014) Graphene-based nanomaterials as heterogeneous acid catalysts: a comprehensive perspective, *Molecules (Basel, Switzerland)*, *19*(9): 14582–14614, DOI:10.3390/molecules190914582

26. Li, Y.F., Guo, M.Q., Yin, S.F., Chen, L., Zhou, Y.B., Qiu, R.H., Au, C.T., (2013) Graphite as a highly efficient and stable catalyst for the production of lactones, *Carbon*, 55: 269-275, DOI:10.1016/j.carbon.2012.12.036

27. Sharghi, H., Hosseini Sarvari, M., (2003) Graphite as an Efficient Catalyst for One-Step Conversion of Aldehydes into Nitriles in Dry Media, *Synthesis, 2:* 243-46, DOI: 10.1055/s-2003-36830

28. Hosseini Sarvari, M., Sharghi, H., (2004) Simple and Improved Procedure for the Regioselective Acylation of Aromatic Ethers with Carboxylic Acids on the Surface of Graphite in the Presence of Methanesulfonic Acid, *Synthesis, 13:* 2165-68, DOI: 10.1055/s-2004-831162

29. Satyen, S., Gautam, P., (2012) Inter- and intramolecularMitsunobu reactionand metal complexation study: synthesis of *S*-amino acids derived chiral 1,2,3,4-tetrahydroquinoxaline, benzo-annulated [9]-N_3peraza, [12]-N_4peraza-macrocycles, *Organic & Biomolecular Chemistry,* 10: 1553-64, DOI: 10.1039/C1OB06304A

30. Saurav, B., Krishnananda, S., Gautam, P. (2011) Unprecedented formation of benzo[d][1,2,3,6]oxatriazocine derivatives via diazo-oxygen bond formation and synthesis of enantiomerically pure 1-alkyl benzotriazole derivatives, *Tetrahedron Letters*, 52(25): 3234-3236, DOI: 10.1016/j.tetlet.2011.04.049

31. Glisoni, R., Gris, J., Fabian, L., Fernandez, B., Moglioni, A., (2008) New Synthetic Methodologies Pointing to Improve the Classical Hinsberg Reaction ,*Tetrahedron Letters*, 49, 6, 1053-1056, DOI:10.1016/j.tetlet.2007.11.204

32. Halgren, T. A. (1999) MMFF VI. MMFF94s option for energy minimization studies. *Journal of Compuational Chemistry.*, 20: 720-729, DOI:10.1002/(SICI)1096-987X(199905)20:7<720::AID-JCC7>3.0.CO;2-X

33. Geldenhuys, W.J., Gaasch, K.E., Watson, M., Allen, D.D., Van der Schyf, C.J., (2006) Optimizing the use of open-source software applications in drug discovery, *Drug Discovery Today*, 127-132, DOI: 10.1016/S1359-6446(05)03692-5

34. Trott, O., Olson, A. J., (2010) AutoDockVina: Improving the speed and accuracy of docking with a new scoring function, efficient optimization, and multithreading, *Journal of Computational Chem*istry, 31: 455-461, DOI:10.1002/jcc.21334

35. Todeschini R, Gramatica P., New 3D molecular descriptors: the WHIM theory and QSAR Applications, 3D QSAR in drug design: Springer, 1998:355

36. Yap, C. W., (2011) PaDEL-descriptor: An open source software to calculate molecular descriptors and fingerprints, *Journal of Computational. Chemistry*, 32: 1466-1474, DOI:10.1002/jcc.21707

37. Boyer, P.L., Clark, P.K., Hughes, S.H., (2012) HIV-1 and HIV-2 reverse trasncriptase: different mechanisms of resistance to nucleoside trasncriptase inhibitors, *Journal of Virology,* 86(10): 5885-5894, DOI:10.1128/JVI.06597-11

Highlights

- A quinoxaline library was constructed and evaluated using docking and 3D-QSAR.
- Twenty-five quinoxaline derivatives were selected and synthesized.
- All compounds were screened for their *in vitro* RT inhibitory activity.
- Four compounds were evaluated as anti-HIV agents in infected MT2 cells.
- Compounds **12** and **3** showed promising anti-HIV activities.

Declaration of interests

X The authors declare that they have no known competing financial interests or personal relationships that could have appeared to influence the work reported in this paper.

☐ The authors declare the following financial interests/personal relationships which may be considered as potential competing interests: